A STUDY OF SYSTEMIC INFLAMMATION AND BROWN ADIPOSE CELLS EMBEDDED IN VISCERAL ADIPOSE OF OBESE PATIENTS

by

Maria Ashley Keaton

A Thesis
Submitted to the
Graduate Faculty
of
George Mason University
in Partial Fulfillment of
The Requirements for the Degree
of
Master of Science
Biology

Committee:

_____	Dr. Ancha Baranova, Thesis Director
_____	Dr. Aybike Birerdinc, Committee Member
Karl J. Fryxell	Dr. Karl Fryxell, Committee Member
James D. Willett	Dr. James D. Willett, Director, School of Systems Biology
Donna M. Fox	Dr. Donna M. Fox, Associate Dean, Office of Academic Affairs and Special Programs, College of Science
P. Agouris	Dr. Peggy Agouris, Dean, College of Science
Date: 5/30/2014	Summer Semester 2014 George Mason University Fairfax, VA

A Study of Systemic Inflammation and Brown Adipose Cells Embedded in Visceral Adipose of Obese Patients

A Thesis submitted in partial fulfillment of the requirements for the degree of Master of Science at George Mason University

by

Maria Ashley Keaton
Bachelor of Science
James Madison University, 2010

Director: Ancha Baranova, Professor
Department of Biology

Summer Semester 2014
George Mason University
Fairfax, VA

DEDICATION

This is dedicated to my generous friends and family, for all of their support through this educational journey.

ACKNOWLEDGEMENTS

I would like to thank the many people who have assisted me in completing this work. I wish to thank Dr. Ancha Baranova, my advisor in this process, her optimism and ambition truly inspires all around her. A special thanks to Katie Doyle, Dr. Aybike Birerdinc, Dr. Rohini Mehta, Dr. Michael Estep, and Dr. Karl Fryxell for their guidance in the laboratory and in my writing and especially to Lei Wang for advising and helping with the statistical analyses. Additional thanks also go out to Dr. Younossi and the staff at the Betty and Guy Beatty Center for Integrated Research at INOVA Fairfax Hospital because without this facility many integral studies, like this one, could not have been realized. Also, I cannot forget Diane St. Germain, thank you for your kindness and support from my first visit to George Mason University.

TABLE OF CONTENTS

Page

List of Tables vii

List of Figures viii

Abstract ix

Introduction 1

- Adipose Tissue 1
- Liver Function 6
  - Energy Balance 6
  - Consequences of Obesity 7
  - Cytokines and Adipokines 7
- Cross Talk between Adipose and other Human Tissues 8
  - T-cell Response 9
  - KCNRG 11
  - TIMP-1 11
  - COL1A1 12
  - Inflammatory related Progression of Diseases associated with Obesity 12
- Study Aims 14

Materials and Methods 15

- Sample Collection 15
- Primer Design and Validation 16
- RNA Extraction from Visceral Adipose Tissues (VAT) 18
- cDNA Synthesis 19
- qRT-PCR/Gel Electrophoresis 20
- Bio-Plex™ Magnetic Bead Assays 21
- Statistics 22

Results 23

Discussion 43

Adipose Tissue 43
Pro-inflammatory Mediators 44
Anti-inflammatory Mediators 46
Limitations of Current Study 49
Conclusions 51
References 52

LIST OF TABLES

Table Page
Table 1 Description of adipokines, cytokines, and transcription factors in this study 10
Table 2 Cohort Demographics 14
Table 3 Primer Descriptions 147
Table 4 Mean and standard deviation of variables in this study 29
Table 5 Spearman's correlations analysis for BMI and the levels of glucose and HDL .. 30
Table 6 Spearman's correlations analysis for CSF-1, CSF-1R, KCNRGv1, KCNRGv2. 32
Table 7 Spearman's correlations analysis for TGF-β1, TIMP-1, COL1A1, TGF-β1R 34
Table 8 Spearman's correlations analysis for PRDM16, UCP1, TBX21, CD3E 35
Table 9 Spearman's correlations analysis for GATA3, FOXP3, IL-1β, IL-2 37
Table 10 Spearman's correlations analysis for IL-4, IL-5, IL-6, IL-7 39
Table 11 Spearman's correlations analysis for IL-8, IL-10, IL-12, IL-13 40
Table 12 Spearman's correlations analysis for IL-17, G-CSF, GM-CSF, IFN-γ 41
Table 13 Spearman's correlations analysis for MCP-1, MIP-1b, TNF-α, TGF-β1 42

LIST OF FIGURES

Figure Page
Figure 1 Inflammatory effects of increased volumes of visceral adipose tissue 5
Figure 2 Fold change of relative gene expression in adipose for NAFLD to No Disease 24
Figure 3 Fold change of relative gene expression in adipose for NASH/No Disease 25
Figure 4 Fold change of relative gene expression in adipose for NAFLD/Non NAFLD. 26
Figure 5 Fold change of relative gene expression in adipose for NASH/Non NAFLD ... 27
Figure 6 Fold change of relative gene expression in adipose for NASH/NAFLD 28

ABSTRACT

A STUDY OF SYSTEMIC INFLAMMATION AND BROWN ADIPOSE CELLS EMBEDDED IN VISCERAL ADIPOSE OF OBESE PATIENTS

Maria Ashley Keaton, M.S.

George Mason University, 2014

Thesis Director: Dr. Ancha Baranova

Obesity has become a major epidemic, not just in the US, but in many other industrialized nations around the world. Obesity has risen due to the natural conflict between availability of calorie-rich foods and energy efficient metabolisms naturally selected for tens of thousands of years in the past. Unfortunately, obesity is detrimental to health as it is associated with a number of chronic conditions including type II diabetes and liver disease. This study explores the effects of the accumulation of visceral adipose on systemic inflammation as measured within adipose itself, in circulation, and in the liver parenchyma as determined by histopathology. The cross-talk between omental deposits of adipose and liver was analyzed by profiling serum cytokine levels, adipose gene expression, and liver biopsy histopathology for 241 morbidly obese patients undergoing bariatric surgery. We showed that the levels of pro-inflammatory cytokines increase in parallel with an increase in the severity of liver disease, while the levels of anti-inflammatory factors decrease. Additionally, we studied expression levels of genes that define the differentiation and activity of brown adipose cells within visceral adipose

collected from the same cohort of morbidly obese subjects. We showed that expression levels for genes specific for brown adipose tissue decrease proportionally to the increase in both serum and histological indicators of systemic inflammation. Importantly, our study is the first to provide evidence that scattered brown adipocytes may be present in visceral adipose of morbidly obese subjects and that their numbers or activity levels may diminish with an increase in systemic inflammation associated with obesity and metabolic syndrome.

INTRODUCTION

Adipose Tissue

Adipose tissue is the major endocrine organ responsible for energy homeostasis. Adipose tissue is composed primarily of adipocytes that are utilized for storing fatty acids in the form of triglycerides, to be broken down during times of low sustenance. In order to maintain a balance in storage verses energy expenditure, adipose relies on a network of signaling molecules, adipokines, to communicate with other tissues in response to changing environmental stimuli.

The increasing prevalence of obesity over the last decades has captured the focus of many researchers. In fact, within the last two decades from 1990 to 2008 the amount of individuals reported as obese has been doubling, going from 11.1% - 26.8% as determined by Body-Mass Index (BMI > 30) (Finkelstein et al., 2012). Even conservative linear projections are predicting that at least 42% of Americans will be obese by 2030 (Finkelstein et al., 2012).

Unfortunately, health complications arise from such an excess of body fat. The expanding adipose tissue can cause hypoxic conditions leading to dysregulation of adipokines (Hosogai et al., 2007). The death of these adipocytes attracts macrophages to the site to "scavenge" the remains where they fuse together, forming a syncytia, seen in most cases of chronic inflammation and increased expression of tumor necrosis factor

(TNF-α) (Cinti et al., 2005). Syncytia are believed to secrete elevated amounts of cytokines causing further macrophage amassing (Gutierrez et al., 2009). However, many state that T-lymphocyte infiltration to the site of adipose inflammation is the first step to macrophage recruitment leading to insulin resistance (Kintscher et al., 2008). Fat accumulation is also suspected of leading to adipose infiltration within the liver leading to nonalcoholic fatty liver disease (NAFLD). The levels of steatosis within NAFLD can progress into nonalcoholic steatohepatitis (NASH) and eventually cirrhosis. These consequences along with type II diabetes go hand in hand with more sedentary, higher caloric lifestyles experienced in many developed and developing countries, and are predominantly seen in obese individuals, thus, forming a vicious pro-inflammatory cycle.

However, fat does not accumulate in the same fashion in everyone nor does it have the same effect on health. Importantly, functional activity of fat depends on its anatomical location, just below the skin (subcutaneous) versus within the abdominal cavity (visceral) (Cinti, 2012). Fat distribution patterns are heavily dependent upon a person's genotype, according to a study of heritability (h^2) of body fat mass and distribution between monozygotic and dizygotic twins (Malis et al., 2005). It has recently been suggested that the highly active visceral adipose may act like an endocrine organ in terms of its systemic signaling patterns (McGown et al., 2014), as increases in BMI are associated with higher levels of both insulin resistance and overall inflammatory signaling.

In essence, since visceral adipose tissue (VAT) can be considered an endocrine organ, like any organ, it is composed of multiple different cell types, some that comprise

the normal body of an organ, and others, like macrophages, dependent on a given environmental stress or biological activity. Adipocytes themselves may be classified as white or brown, and in specific cases, where the cell phenotypes are ambiguous, they may be identified as beige or "brite" as well.

Until recently, the classical paradigm suggested that, in adult humans, adipose tissue is represented only by white adipocytes. However, more recent studies have shown masses of metabolically active brown adipocytes in the supraclavicular region (Nedergaard et al., 2007; Virtanen et al., 2009). In rare instances, brown adipose depots were also found spanning the m. subscapularis to the m. pectoralis regions (Bjorndal et al., 2011; Cypess et al., 2009). Despite these discoveries, the exact purpose of brown adipose tissue (BAT) in adult humans has yet to be elucidated. More is known about the role of BAT in infancy, when the human body regulates its temperature through an excessive production of heat through BAT-dependent non-shivering thermogenesis (Lean et al., 1986; Townsend and Tseng, 2012).

Brown adipocyte thermogenesis is mediated by uncoupling protein 1 (UCP1) that uncouples oxidative phosphorylation and adenosine triphosphate (ATP) production (Cannon and Nedergaard, 2004). This process takes place in the numerous multilobular mitochondria found in BAT, which give these cells their characteristic brown coloration. The expression of UCP1 protein can be induced by transcription factor PR domain containing 16 (PRDM16) that promotes differentiation of BAT from the progenitor cells. Interestingly, after stimulation with some PPARγ ligands, white adipocytes may be

transdifferentiated into the so-called “brite” (brown/white) or beige cells (Petrovic et al., 2010; Wu et al., 2012).

White adipose tissue (WAT), on the other hand, stores fat as triglycerides which can be released later for use as a source of energy throughout the body. In the last decade, the understanding of the function of WAT has greatly been expanded from a simple energy storage milieu to a highly active endocrine organ with far reaching targets (McGown et al., 2014). The presence of excess amounts of white visceral adipose widely known as obesity are associated with metabolic syndrome (Cinti, 2009, 2012). WAT secrets many cytokines, hormones and hormone-like proteins, including leptin, adiponectin, TNF-α, IL-6, resistin and others which regulate energy homeostasis, cell death, and immune response. In metabolic syndrome, the on-set of insulin resistance due to increased abdominal mass commonly leads to further pathophysiological complications such as type II diabetes, heart disease that results from hypertension and detrimental shifts in serum lipid composition, arthritis, and even tumorigenesis. It is suggested that the pro-inflammatory shift of the ratio of TNF-α-like cytokines to anti-inflammatory cytokines takes place in visceral adipose, and that this shift is to blame for a compromised sensitivity to insulin throughout the tissues (Gutierrez et al., 2009) (Figure 1).

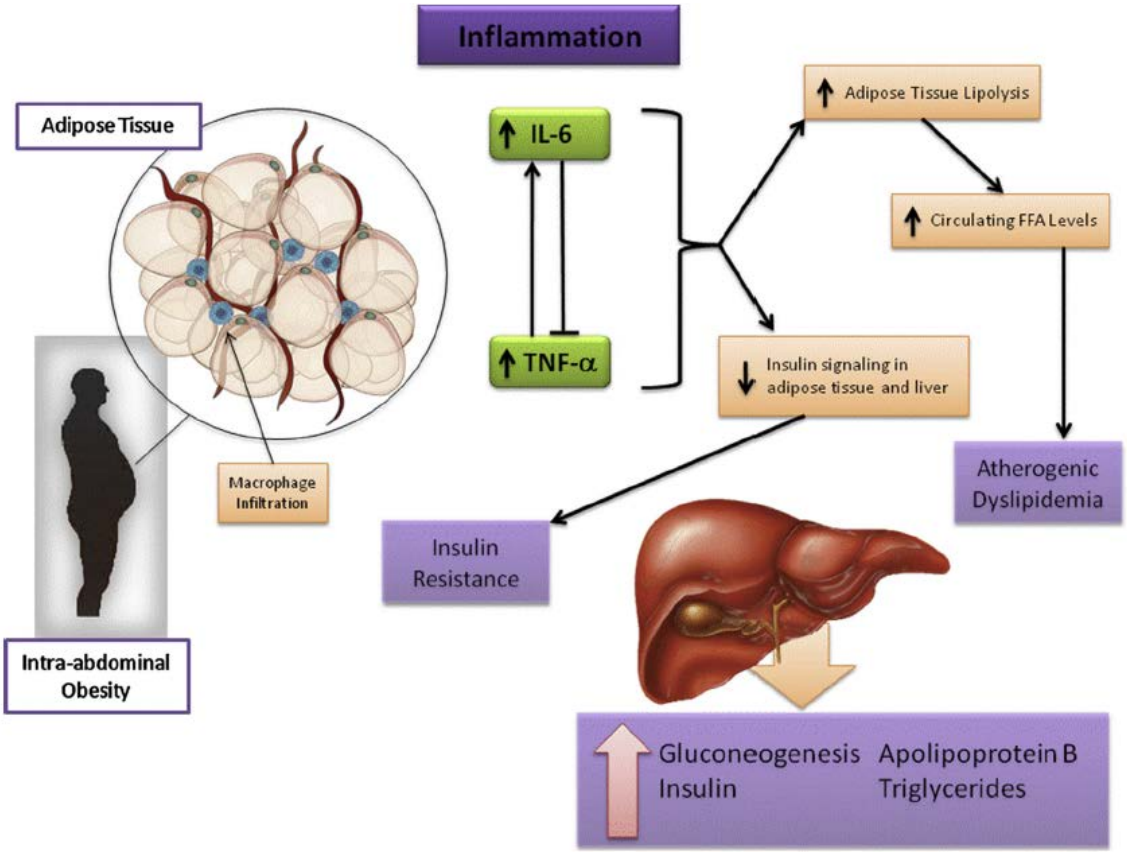

Figure 1 Downstream inflammatory effects of increased volumes of visceral adipose tissue. Courtesy of Dr. Ancha Baranova and Dr. Aybike Birerdinc.

Interestingly, recent research suggests that the activity of BAT may aid in counterbalancing some of the deleterious effects of metabolic syndrome through assisting the uptake and expenditure of excess glucose and free fatty acids as heat, while increasing metabolic rate and decreasing insulin resistance (Orava et al., 2011; Townsend and Tseng, 2012). Hence, there is an increase in the exploration of the function of brown fat now seen as the "neglected jewel" in studies of adipose signaling and the regulation of metabolism (Birerdinc et al., 2013).

Liver Function

The liver is composed of cells known as hepatocytes. Under normal conditions of relatively low background inflammation, the liver functions to store glucose in the form of glycogen. Hepatocytes store glycogen till it is called upon and released into the bloodstream and catabolized to pyruvic acid, to produce ATP in the mitochondria. Additionally, free fatty acids are synthesized *de novo*, or up-taken into the liver, where they may be stored or utilized to produce phospholipids, triglycerides, cholesterol, and lipoproteins.

Energy Balance

Both the liver and adipose possess the ability to sequester excessive amounts of nutrients during times of abundance; hence, both of these tissues are fundamental to our survival. In the abundant caloric environment of a post war/industrialized era, the efficiency of our metabolism is now augmenting the environmental detriment to our bodies (Bellisari, 2008).

This trend was documented by a WHO MONICA study that cross-referenced national food supply with data on BMI from 34 populations in 21 countries from 1980 to the mid '90s (Silventoinen et al., 2004). Interestingly, while BMI increased in Western European countries, Australia, the USA, and China there was a decrease in BMI in Central and Eastern European countries (Silventoinen et al., 2004). These fluctuations in BMI correlated with increase or decrease in total energy supply *per capita*, respectively (Silventoinen et al., 2004). In fact, 41% of the variation in mean BMI, as well as the

prevalence of those overweight and obese, were explained by total energy supply *per capita* (Silventoinen et al., 2004).

Consequences of Obesity

As our bodies begin accumulating fat, the central depot of excess energy, there comes a point at which the liver is no longer capable of keeping up with the demands of the body. Although it is still unclear how and when the adverse effects begin, we do know that the risk of developing non-alcoholic fatty liver disease (NAFLD) increases with BMI. However, not everyone, even some of those who are morbidly obese, has any liver disease. Overall, the trends in populations indicate that the accumulation of excessive adipose results in an increased incidence of fatty liver disease and its complication, non-alcoholic steatohepatits (NASH) (Luyckx et al., 2000). Yet, not everyone develops NASH either, and it is still unclear how fatty liver disease (steatosis) progresses to NASH. It is clear, however, that both of these ailments are linked to insulin resistance, possibly due to a disturbance of insulin signaling by overactive immune cells. This "runaway" immune response is characterized by the loss of Treg cells, which normally help to balance/regulate Th1/Th2 T-lymphocytes in the visceral adipose (Feuerer et al., 2009). In turn, the deregulation of Th1/Th2 T-lymphocyte balance leads to a damage to the hepatocytes, and a loss in the efficiency of liver function (Mirza, 2011).

Cytokines and Adipokines

Within an organism, cells communicate through an array of soluble signaling molecules. These extracellular proteins are classified according to the distance they travel from their "home" cell to the "receiving/destination" cell. Autocrine molecules only act on the "home" cell, while paracrines can act on both "home" and distant cells, thus, exerting a systemic effect.

Due to its active role in distant signaling through the secretion of adipokines, adipose has been established as an active endocrine organ that is no longer viewed as a dormant tissue utilized as an energy storage (McGown et al., 2014). Adipokines and cytokines are the primary activators of inflammation and insulin resistance during obesity (Kang et al., 2013). For example, serum levels of resistin correlate to BMI amongst postmenopausal, Indian women (Sadashiv, 2012). Many adipokines have been shown to influence the expression of cytokines and inflammation throughout the body, as is the case of adiponectin.

Apidonectin is unique in a sense; its levels are lower during obesity (Arita et al., 1999), but can be increased by aerobic exercise, although this is also dependent upon genetic factors (Lee et al., 2013). Adiponectin works in an anti-inflammatory manner by increasing the expression of IL-10 and IL-1RA (Goktas et al., 2013), while decreasing the levels of C-reactive protein, a marker of inflammation (Ahonen et al., 2012).

Cross Talk between Adipose and other Human Tissues

Recent studies shed some light on the influence of adipose tissue on other organs and how it affects the entire body of obese individuals. Adipose is a highly vascularized tissue that is capable of siphoning adipokines and cytokines to and from this organ and

throughout the body and to adjacent organs such as the stomach, liver, heart, and pancreas (Cao, 2014; McGown et al., 2014). Transforming growth factor beta 1 (TGF-β1) is mainly secreted by blood platelets, and contributes to macrophage accumulation at the site of injury/inflammation (Wahl et al., 1990). Its levels are increased in obese individuals. Within adipose, the macrophages are the primary source of (TGF-β1) and are embedded in the adipose tissue, rather than the fat cells itself (Fain et al., 2005). TGF-β1 is shown to influence the expression of other cytokines. In a study of mRNA expression induced by TGF-β1 in the murine T-cell line EL4, a significant up-regulation of IL-2 was observed (Han et al., 1998). The infiltration of TGF- β producing macrophages into visceral adipose may interfere with the differentiation of resident immune cells.

T-cell Response

In the human immune system, T-helper cells are able to differentiate into two lymphocyte subsets: Th1 and Th2. Under unperturbed conditions, T-cell types regulate one another through cytokine signaling. Cytokines IL-4, IL5, and IL10 promote the differentiation of Th2 cells, while other cytokines such as IL-2, IFN-γ, and TNF-β encourage the production of Th1 cells. The cytokines IL-4 and IFN-γ reciprocally inhibit the proliferation of the other lineage, thus maintaining a balance between the two cell populations (O'Garra, 1998). In the nuclei, differentiation of these two lineages is governed by two transcription factors: TBX21 and GATA-3. GATA-3 controls the expression of IL-4 in Th2 cells, while TBX21 regulates IFN-γ transcription in Th1 cells (Szabo et al., 1997; Zheng and Flavell, 1997). These two T-helper lymphocyte subsets

are also regulated by Treg cells which differentiate through an up-regulation in the transcription factor FOXP3. The hypoxic, apoptosis inducing environment in adipose of obese individuals induces the expression of adipokines that may directly influence the differentiation of T cells.

Table 1 Description of adipokines, cytokines, and transcription factors profiled in this study.

Protein Name	**Description**
IL-1β	Interleukin 1 pro-inflammatory cytokine produced by macrophages.
IL-2	Interleukin 2 is a cytokine that promotes T and B lymphocyte proliferation.
IL-4	Interleukin 4 is a cytokine secreted by active Th2 cells.
IL-5	Interleukin 5 is a pro-inflammatory cytokine that proliferates B cells and eosinophils.
IL-6	Interleukin 6 is a pro-inflammatory cytokine involved in the maturation of B cells.
IL-7	Interleukin 7 is a cytokine involved in the development of T and B cells.
IL-8	Interleukin 8 is a pro-inflammatory chemokine of the CXC family.
IL-10	Interleukin 10 is an anti-inflammatory cytokine produced mostly be monocytes.
IL-12	Interleukin 12 is a pro-inflammatory cytokine that induces the expression of IFN-γ.
IL-13	Interleukin 13 is an anti-inflammatory cytokine produce by Th2 cells.
IL-17	Interleukin 17 is a pro-inflammatory cytokine produced by T cells.
G-CSF	A granulocyte colony stimulating factor cytokine.
GM-CSF	A macrophage colony stimulating factor cytokine.
IFN-γ	Type II interferon gamma is an immunoregulatory cytokine.
MCP-1 (CCL2)	Pro-inflammatory cytokine, part of the CC chemokine superfamily.
MIP-1β	Macrophage inflammatory protein cytokine produced by macrophages.
TNF-α	Tumor necrosis factor proinflammatory cytokine.
TGF-β1	Transforming growth factor beta inhibitory cytokine.
CD3E	Component of the T-cell surface receptor CD3 complex.
FOXP3	Forkhead/winged-helix family transcription factor for Treg cells. (IL-10, TGF-β)
TBX21	Transcription factor for Th1 cells that contains a T-box, DNA binding domain. (IFN-γ)

GATA3	A GATA-type zinc finger transcription factor for Th2 cells (IL-4, IL-13)

These cytokines both influence the differentiation of T-lymphocytes and are being produced by T-cells and other immunity components (Table 1). Other genes in Table 1 have been recognized for their important roles in cell cycle and energy homeostasis pathways and may also be involved in the diseases of the deregulation of adipose tissue signaling.

KCNRG

Potassium channel regulating gene (KCNRG) belongs to an incompletely studied gene family of KCTD that encodes the domain similar to the T1 (tetramerization) domain of the Kv potassium channels. A protein-protein interaction study implicated KCTD family protein KCTD15 in energy homeostasis through the suppression of apidogenesis (Mikhail Skoblov, 2013). KCNRG-encoded proteins help suppress potassium currents by possibly interfering with their assembly (Birerdinc et al., 2010). When overexpressed, KCNRG has been shown to suppress cell growth while encouraging apoptosis in a number of tumor cell lines (Birerdinc et al., 2010). It was hypothesized that KCNRG and/or other members of KCTD family may also play a role in adipose cell apoptosis and regulation of pro and anti-inflammatory signaling.

TIMP-1

Tissue inhibitor of metalloproteinases-1 (TIMP-1) is a known biomarker of macrophage infiltration in adipose tissue. TIMP-1 plays a role in down-regulation of

angiogenesis. During differentiation, macrophages up-regulate matrix metalloproteinase-9 (proMMP-9), thus contributing to angiogenesis. In agreement with this fact, proMMP-9 and TIMP-1 producing macrophages become polarized to M2 without the occurrence of angiogenesis, while null TIMP-1, normal proMMP-9 producing macrophages (M0, M1, and M2) support angiogenesis (Zajac et al., 2013).

COL1A1

Collagen I (COL1A1) is an extracellular matrix structural protein. The presence of collagen, usually produced by fibroblasts, is a biomarker of the fibrosis that disrupts the architecture and the function of liver parenchyma. Up-regulation of collagen I has been seen in both pulmonary and liver fibrosis through the activation of the Wnt pathway (Miao et al., 2013). Recently it has been implicated in glomerulosclerosis, where glomerular cells lose function by becoming displaced by excess amounts of collagen (Hornigold et al., 2013). Type I collagen biosynthesis is stimulated by a number of pathways. In particular, in human vascular smooth muscle cells (VSMCs), TGF-β has been shown to induce the expression of collagen of both type I and type III (Amento et al., 1991). An increase in inflammation and in macrophage infiltration during obesity stimulates the local secretion of TGF-β1 that, in turn, may increase collagen production and propagation of fibrosis in the liver or other organs.

Inflammatory related Progression of Diseases associated with Obesity

Obesity-associated adipose tissue inflammation is a major cause of the decreased insulin sensitivity seen in type 2 diabetics. In a study of C-C motif chemokine receptor–

2 (CCR2), a high affinity receptor for circulating CCL2 (MCP-1), it was discovered that *CCR2* knock-out mice fed with a high fat diet showed a delayed onset of obesity due to *CCL2* deficiency (Weisberg et al., 2006). These mice also had reduced macrophage infiltration and inflammation in the adipose tissue, while maintaining relatively high levels of adiponectin production, lesser degree of hepatic steatosis, and enhanced systemic insulin sensitivity (Weisberg et al., 2006).

It is well recognized that the deposits of fat, especially within visceral adipose, greatly contribute to establishing systemic background inflammation triggered by the release of adipokines, like IL-1β (Cipolletta et al., 2011). In turn, IL-1 family molecule overproduction can throw off the Th1/Th2 cell balance, and, in some cases, causes preferential differentiation of Th2 cells resulting in an inflammatory and allergic response (O'Garra, 1998). These cytokines, including monocyte chemoattractant protein-1 (MCP-1), attract macrophages and contribute to local inflammation by stimulating the release of other pro-inflammatory proteins (Kintscher et al., 2008).

Currently, the factors involved in the progression from NAFLD to NASH are still unknown (McGown et al., 2014). Although the correlative evidence indicates that adipose tissue signaling drives this process. For example, the fluctuations of adiponectin levels in visceral adipose tissue are highly correlated with serum levels of free fatty acids and severity of steatosis (Valenti et al., 2012). The progression of steatosis into NASH is typically accompanied by an increase in liver fibrosis through the up-regulation of collagen production around the portal triads and pericellular regions within the liver parenchyma.

Study Aims

To support the idea of visceral adipose tissue as an endocrine organ, we will examine adipose tissue, composed of a phenotypically diverse community of cells, and its involvement in the release of signaling molecules that affect cell expression and differentiation. We believe that the cytokines released by adipose tissue impact the degree and severity of liver disease seen in morbidly obese individuals. A cohort of 241 morbidly obese patients was selected for this study (Table 2).

Table 2 Cohort Demographics

Description	**Adipose samples, n = 84**	**Serum samples, n = 241**	**Liver Biopsies, n=233**
Age	43.43 ± 11.73		
BMI	46.39 ± 10.91		
Females	75.0% (180)		
Males	25.0% (60)		
Diabetes	28.6% (68)		
No Liver Disease	22.3% (52)		
Non-NAFLD Liver Disease	4.7% (11)		
NAFLD (Non-NASH)	33.9% (79)		
NASH	39.1% (91)		
Cirrhosis	3.5% (8)		

MATERIALS AND METHODS

Sample Collection

This study was approved by INOVA Internal Review Board. The visceral adipose samples were collected from patients during elective gastric bypass surgery at INOVA Fair Oaks Hospital. Samples were snap frozen and transferred on dry ice to INOVA Fairfax Hospital. Whole blood samples were collected at INOVA Fairfax Hospital and immediately processed to separate out the serum. All samples were de-identified in compliance with HIPAA regulations.

NAFLD spectrum diseases were diagnosed by obtaining a needle core biopsy. For histopathological evaluation, each sample was formalin-fixed, sectioned, and stained with hematoxylin-eosin and Masson trichrome. Slides were reviewed by a single hapatopathologist according to the established histologic grading system. Histological parameters evaluated include portal inflammation, lymphoplasmacytic lobular inflammation, polymorphonuclear lobular inflammation, Kupffer cell hypertrophy, apoptotic bodies, focal parenchymal necrosis, glycogen nuclei, hepatocellular ballooning, and Mallory-Denk bodies. Samples that demonstrated hepatic steatosis (with or without non-specific inflammation) or NASH were considered to be NAFLD. NASH was defined as steatosis, lobular inflammation, and ballooning degeneration with or without Mallory Denk bodies, and with or without fibrosis (Bondini et al., 2007).

Primer Design and Validation

The primers for mRNAs encoding UCP1, PRDM16, KCNRGv1, KCNRGv2, FOXP3, TBX21, CD3E, and GATA3 (Table 3) were designed using the NCBI Primer BLAST tool. Parameters were set to amplify products between 70-300 bp, thus, allowing for the identification of primer dimers and contaminating genomic templates. Primer pairs were also specified to cross exon-exon boundaries, and span at least one intron, when possible. These criteria were adjusted when search returned unacceptably poor choices. Primers were selected based on their annealing temperatures, preferably at 60°C, and low self-complementarity to avoid the formation of secondary structures and self-binding. The selected primers were synthesized by the Invitrogen™ Custom DNA Oligos (Life Technologies, Grand Island, NY, USA). Primers for TGF-β1, TGF-β1R, ACTβ, TIMP-1, CSF-1, CSF-1R, and COL1A1 were selected from pre-validated primer sets from Real Time Primers LLC (Table 3).

To validate the formation of proper PCR products, all primer pairs were initially validated on universal cDNA samples, reverse transcribed from XpressRef^{TM} Human Universal Reference Total RNA (SABiosciences, QIAGEN, Valencia, CA, USA) before being tested on cDNA prepared from the samples comprising of the cohort (data not shown).

Table 3 Primer Descriptions

Invitrogen	Sequences (5'-3')	Temp	Size
UCP1	F: TCTCTCAGGATCGGCCTCTA R: GCCCAATGAATACTGCCACT	60	127 bp
Exon Region:	344-470 bp	NM_021833.4	
PRDM16	F: TGAGAAGTTCTGCGTGGATG R: GCTTGGACTGGAAGAGTTCG	60	269 bp
Exon Region:	541-809 bp	NM_022114.3	
KCNRGv1	F: TTTTCCCTCCTCAGATGACC R: TCCAGTTTGGTTATCAGTAGTGC	60	107 bp
Exon Region:	707-813 bp	NM_173605.1	
KCNRGv2	F: CCTGGTTTTCCAGTGTG R: GCTGAGGCAGGAGAATCACT	60	129 bp
Exon Region:	765-893 bp	NM_199464.2	
FOXP3	F: GAAACAGCACATTCCCAGAGTTC R: ATGGCCCAGCGGATGAG	60	100 bp
Exon Region:	1138-1237 bp	NM_014009.3	
TBX21	F:TGTTGTGGTCCAAGTTTAATCAGCA R: CCCGGCCACAGTAAATGACAG	60	95 bp
Exon Region:	645-739 bp	NM_013351.1	
CD3E	F: GATGCAGTCGGGCACTCACT R: CATTACCATCTTGCCCCCA	60	77 bp
Exon Region:	256-332 bp	NM_000733.3	
GATA3	F: CGAGATGGCACGGGACACTA R: TGGTCTGACAGTTCGCACAGG	60	142 bp
Exon Region:	1386-1527 bp	NM_001002295.1	
RealTimePrimers.com	**Sequences (5'-3')**	**Temp**	**Size**
TGF-β1	F: CGT GGA GCT GTA CCA GAA ATA R: TCC GGT GAC ATC AAA AGA TAA	58°C	106 bp
Exon Region:	1368-1473 bp	NM_000660	
TGF-βR1	F: GAA GAA TGG AAG CAG TGC AA R: CTC CCC GAA CAC GCT ATA AT	58°C	200 bp
Exon Region:	5893-6092 bp	NM_004612	
ACTβ	F: GGA CTT CGA GCA AGA GAT GG R: AGC ACT GTG TTG GCG TAC AG	58°C	234 bp
Exon Region:	736-969 bp	NM_001101.2	
TIMP-1	F: TAC TTC CAC AGG TCC CAC AA R: ATT CCT CAC AGC CAA CAG TG	58°C	166 bp
Exon Region:	475-640 bp	NM_003254	
CSF-1	F: CCC AGT GTC ATC CTG GTC TT R: GAG ACT GTT CTG TGC GTC CA	60°C	193 bp
Exon Region:	1696-1888 bp	NM_000757	
CSF-1R	F: GTG GCT GTG AAG ATG CTG AA R: CCT TCC TTC GCA GAA AGT TG	60°C	199 bp
Exon Region:	2129-2327 bp	NM_005211	

COL1A1	F: GGA CAC AGA GGT TTC AGT GG R: CCA GTA GCA CCA TCA TTT CC	60°C	191 bp
Exon Region:	3841-4090 bp	NM_000088	

RNA Extraction from Visceral Adipose Tissues (VAT)

Total RNAs were extracted from VAT samples using Aurum™ Total RNA Fatty and Fibrous Tissue Kit (BioRad Laboratories, Hercules, CA, USA). Previously collected visceral adipose samples, stored in a -80˚C freezer, were cut into 100 mg portions with a scalpel and suspended in 2 ml centrifuge tube with 1 ml of PureZOL™ RNA Isolation Reagent (Bio-Rad Laboratories, Hercule, CA, USA). PureZOL lyses the cells and aids in the homogenization, the latter process was performed using the Fisher Scientific™ PowerGen™ Model 125 Homogenizer (Fisher Science Education, Hanover Park, IL, USA). Cell disruption was followed with a 5 minute incubation at room temperature. The lysate was then centrifuged at 12,000 x g for 10 minutes at 4˚C and the supernatant was transferred into a new 2 ml tube. 0.2 ml of chloroform was added and the tube was shaken rapidly (not vortexed to ensure equal emulsification for phase separation) for 15 seconds. This was accompanied by second room temperature incubation and 12,000 x g, 10 minute spin. The lysate formed three layers, the top, aqueous layer containing the RNA was transferred into a 2 ml tube without the disruption of the DNA containing, intermediate layer below. An equal volume of 70% ethanol was added. 700 µl of RNA sample was added to an RNA mini binding column and centrifuged at 12,000 x g for 60 seconds. 700 µl of low stringency wash was added to each column and centrifuged at 12,000 x g for 30 seconds. Then 700 µl of high stringency wash was added and spun at

12,000 x g for 30 seconds then 700 µl of low stringency wash was added and spun at 12,000 x g for 1 minute. Wash solution was discarded from the wash tube in between every wash step. Then the column was spun an additional 2 minutes at 12,000 x g to remove excess wash buffer. Then samples were eluted in 20 µL of molecular grade water. Spectrometry GE Healthcare GeneQuant^{TM} 1300 Spectrophotometer (Fisher Science Education, Hanover Park, IL, USA) readings and 1% agarose gels with ethidium bromide (Bio-Rad Laboratories, Hercule, CA, USA) was performed in order to ensure quantity and quality respectively, of RNA extraction reactions.

cDNA Synthesis

RNA samples were converted into cDNA for stable storage using RT2 HT First Strand Kit (96) (SABiosciences, QIAGEN, Valencia, CA, USA). 1 µg of total RNA plus molecular grade water was diluted for a total volume of 8 µL. This was mixed with 6 µl of GE2 genomic DNA elimination buffer (SABiosciences, QIAGEN, Valencia, CA, USA) for a final volume of 14 µl. The mixture was briefly centrifuged and incubated at 42˚C for 5 minutes and chilled on ice for 1 minute. 6 µL of BC4 reverse transcriptase master mix buffer (SABiosciences, QIAGEN, Valencia, CA, USA) was added to the RNA mixture for a new volume of 20 µL. This was incubated for 15 minutes at 42˚C and the followed by 5 minutes at 95˚C to stop the reaction. Finally, 91 µl of molecular grade water was added to each tube and thoroughly mixed and stored at -25˚C. These cDNA samples were analyzed for expression levels of mRNA of transcription factors for differentiation of T-helpers cells and for BAT specific gene transcripts using qRT-PCR. Forward and reverse primers were run at a concentration of 250 nM in 10 µl reactions

using SsoFast™ EvaGreen® Supermix (BioRad Laboratories, Hercules, CA, USA) in a 96 well format. All qRT-PCR reactions were performed in the BioRad CFX96 Real Time System (BioRad Laboratories, Hercules, CA, USA).

qRT-PCR/Gel Electrophoresis

Standard qRT-PCR techniques were used to detect mRNA transcripts using Invitrogen™ Custom DNA Oligos (Life Technologies, Grand Island, NY, USA). The qRT-PCR programming was based on the custom primers' individual optimum temperatures. Melting curves were used to validate primer specificity. The real-time PCR mixtures containing 1 ng of cDNA, 250 nM each of forward and reverse primers and SsoFast™ EvaGreen® Supermix (BioRad Laboratories, Hercules, CA, USA) was carried out in a total volume of 10 µl. Reactions were performed in a 96-well format in the BioRad CFX96 Real Time System (BioRad Laboratories, Hercules, CA, USA). Samples were run in triplicate. Using the delta delta (ΔΔ)*Ct* method, the expression values were normalized against the expression of the housekeeping gene ACTβ, previously validated for its stable expression in adipose tissue as a reference gene (Mehta et al., 2010). Due to large sample number, multiple plates were used; an interplate controls, GAPDH and TBP, run at the same RNA sample, served for interplate normalization. PCR protocol was set to BioRad EvaGreen® Supermix specifications and optimum primer temperatures.

Following qPCR, the gel electrophoresis was performed in a 1% agarose gels. To make each gel, the agarose powder was dissolved into 40 mL of TAE buffer with 2 µL of ethidium bromide (10 mg/mL). 1 µL of the qPCR product was mixed with loading dye and run along with 3-10 µL of 100 bp DNA ladder for approximately 50 minutes at 100

V. Bands were visualized under UV light to confirm the product size and quality of qPCR reaction for each primer.

Bio-Plex™ Magnetic Bead Assays

Serum samples from 241 morbidly obese patients were assessed for various biomarkers using two separate Bio-Plex™ assays. The Bio-Plex Pro™ TGFβ assay (BioRad Laboratories, Hercules, CA, USA) was run after diluting the samples to a recommended concentration of 1:16 (5 µL sample and 73 µL sample diluent). For this assay, an additional step is required to activate the target. To do that, into the diluted sample, 1 µL of HCL was added and mixed through pipetting. This mix sat for 10 minutes then 1 µL of NaOH was added to neutralize the mixture. Coupled bead solution, and standards were set up accordingly to the manufacturer' protocol. Briefly, the vortexed beads were plated at 50 µL into each well followed by two washes of 100 µL per well of wash buffer. Next, 50 µL of (1:4) standard, blank, controls, and samples were loaded onto the plate, then the plate was sealed and shaken at 850 rpm for 2 hours. The detection antibody was also diluted according to protocol and added at 25 µL per well after 3 wash cycles. Again the plate was shaken, this time for 1 hour at 850 rpm. 10 minutes into the incubation, the streptavdidin-PE was prepared and added after 3 wash cycles at a volume of 50 µL per well and resealed and shaken for 30 minutes at 850 rpm. 3 more wash cycles and 125 µL of assay buffer was added to each well to re-suspend the beads. After 30 seconds of shaking at 850 rpm the plate was read on the Bio-Plex™ 200 system (BioRad Laboratories, Hercules, CA, USA).

To quantify the panel of pro and anti-inflammatory biomarkers, the Bio-Plex Pro™ Human Cytokine 17-Plex assays (BioRad Laboratories, Hercules, CA, USA) were performed. These assays are similar to the TGFβ assays, except the samples were diluted (1:4); and the first incubation was for 1 hour, the second was for 30 minutes, and the last was shaken at 850 rpm at room temperature for 10 minutes. Lastly, 125 µL of assay buffer was added to each well and the plate was sealed, shaken for 30 seconds and read.

Statistics

In the experiments quantifying the differential expression of the genes and detected cytokine levels standard deviations were large demonstrating substantial variation between individuals expected in a cohort of over 200 patients. Common experience shows that reaching a normal distribution would require an enrollment of an impractically large cohort. To alleviate this problem, non-parametric statistical tests were employed. In particular, non-directional Mann Whitney U tests were performed to determine if two discrete variable groups' means (for example, in comparison of two distinct liver conditions) were significantly different from one another. From the statistically significant means of relative expression, fold changes (FC) were derived as the ratios of each pair compared, (e.g., Mean$\Delta\Delta Ct_{\text{NASH}}$/ Mean$\Delta\Delta Ct_{\text{NoDisease}}$). Spearman's correlation was used to assess the relationship of dependence between continuous variables within the cohort of study. The rho value was also used to calculate the (r^2) coefficient of determination to assess variable *y*'s accountability of variable *x*. All statistical analyses were performed with MATLAB® software.

RESULTS

Adipose and serum samples from 241 morbidly obese patients were analyzed for mRNA and protein expression through qRT-PCR and Bio-Plex techniques, respectively. First, primers were validated at their optimal temperatures with 1 ng of universal human cDNA template and products were run on a 1% agarose gels at 100V (data not shown).

Once the primers were validated, relative mRNA transcript levels within adipose samples were assessed through qRT-PCR. All target gene *Ct*'s were normalized using *ACTβ* as a housekeeping gene. Normalized data were grouped by liver condition as defined by the histopathology reports into "No liver disease", "Non-NAFLD liver disease" (basically encompassing inflammatory or fibrotic changes in absence of steatosis), "Non-NASH NAFLD" (various degrees of non-inflammatory or minimally inflammatory liver steatosis), and "NASH". For select genes, fold differences are shown in Figures 2, 3, 4, 5, and 6.

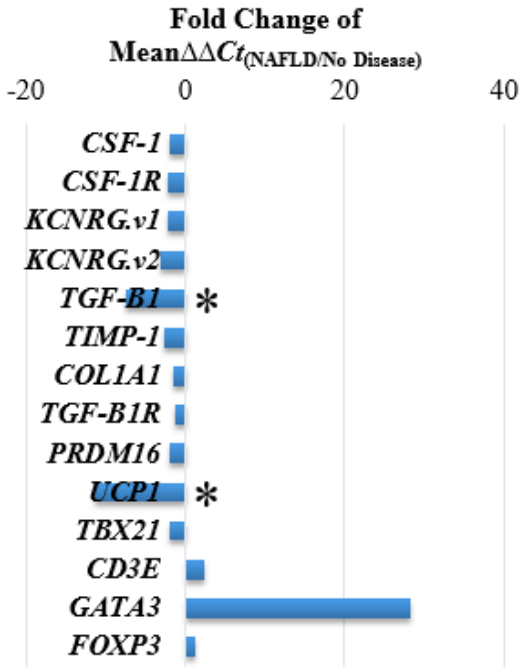

No Disease n= 52	NAFLD n= 79
Mean ± SD	Mean ± SD
3.33 ± 6.23	1.73 ± 2.65
39.26 ± 110.82	18.02 ± 13.53
1.60 ± 1.93	0.73 ± 0.74
0.40 ± 1.44	0.13 ± 0.24
0.82 ± 1.87	0.11 ± 0.17
315.13 ± 840.87	118.08 ± 134.66
73.83 ± 119.17	50.66 ± 41.66
3.63 ± 5.86	2.58 ± 2.88
9.66 ± 15.77	4.94 ± 11.68
58.92 ± 156.45	5.21 ± 18.19
2.60 ± 5.87	1.28 ± 2.03
12.34 ± 19.58	27.94 ± 99.29
3.91 ± 3.36	110.55 ± 536.76
0.54 ± 1.43	0.68 ± 2.09

Figure 2 Fold change between discrete liver statuses of normalized gene of interest expression in adipose, from ACTB expression, for Mean$\Delta\Delta Ct_{NAFLD}$/Mean$\Delta\Delta Ct_{No\ Disease}$. Statistically significant values ($p<0.05$) are indicated (*). Non graphical display of means and standard deviations (SD) for no liver disease and NAFLD (non NASH).

Based upon liver histopathology grouping, the comparison of NAFLD to "no disease" revealed statistically significant differences in the levels of mRNAs encoding for *UCP1* and *TGF-β1*. A comparison of "Non-NAFLD liver disease" to "No liver disease" yielded no significant results (not shown). Interestingly, the mean expression levels of both *UCP1* (Fold change = -11.31, $p<3.8e^{-02}$) and *TGF-β1* (Fold change = -7.39, $p<8.0e^{-03}$) in the adipose tissue were greater in the 'no liver disease' group than the NAFLD group (Figure 2).

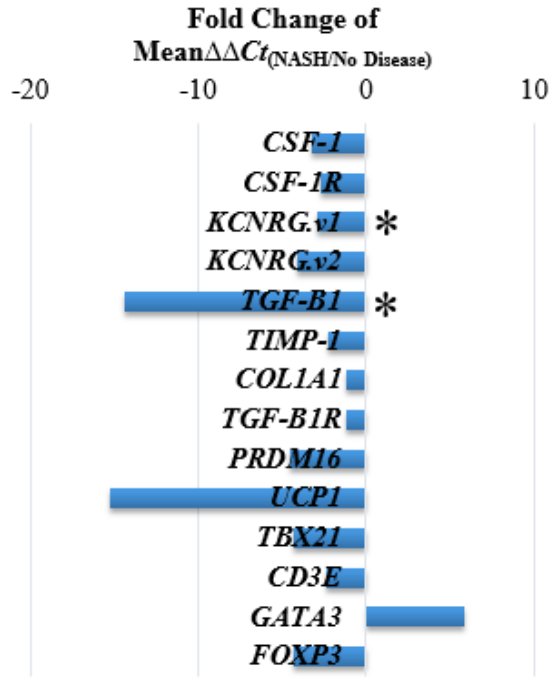

No Disease n= 52	NASH n= 91
Mean ± SD	Mean ± SD
3.33 ± 6.23	1.03 ± 1.46
39.26 ± 110.82	14.55 ± 8.00
1.60 ± 1.93	0.56 ± 0.60
0.40 ± 1.44	0.10 ± 0.24
0.82 ± 1.87	0.06 ± 0.07
315.13 ± 840.87	141.95 ± 118.94
73.83 ± 119.17	62.60 ± 66.02
3.63 ± 5.86	2.96 ± 3.72
9.66 ± 15.77	2.11 ± 4.22
58.92 ± 156.45	3.86 ± 6.12
2.60 ± 5.87	0.61 ± 0.51
12.34 ± 19.58	5.30 ± 5.59
3.91 ± 3.36	22.75 ± 67.77
0.54 ± 1.43	0.12 ± 0.15

Figure 3 Fold change between discrete liver statuses of normalized gene of interest expression in adipose, from ACTB expression, for Mean$\Delta\Delta Ct_{NASH}$/Mean$\Delta\Delta Ct_{No\ Disease}$. Statistically significant values ($p<0.05$) are indicated (*). Non graphical display of means and standard deviations (SD) for no disease and NASH.

When *TGF-β1* mRNA expression levels were compared for NASH group and "No liver disease" group, a significant decrease was seen in NASH patients (Fold change = -14.42, $p<6.8e^{-05}$). Similarly, significant differences were seen for levels of mRNA encoding for *KCNRGv1* (Fold change = -2.87, $p<1.8e^{-02}$); these levels were also significantly lower in those with NASH (Figure 3).

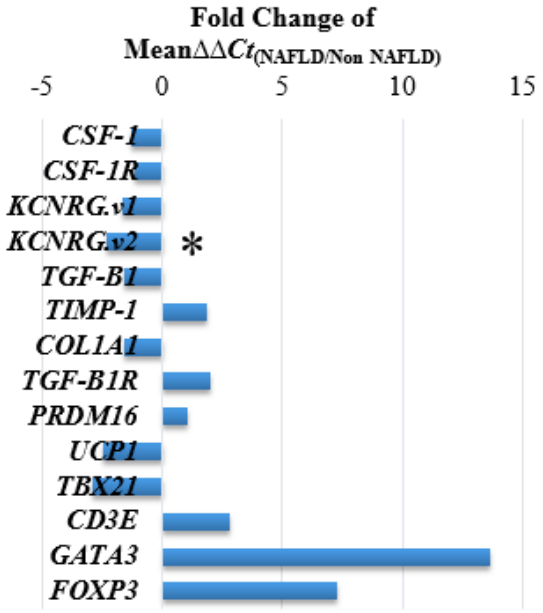

Non-NAFLD n= 11	NAFLD n= 79
Mean ± SD	Mean ± SD
2.28 ± 2.29	1.73 ± 2.65
20.85 ± 9.53	18.02 ± 13.53
1.20 ± 1.59	0.73 ± 0.74
0.30 ± 0.37	0.13 ± 0.24
0.17 ± 0.13	0.11 ± 0.17
63.86 ± 65.14	118.08 ± 134.66
81.53 ± 44.43	50.66 ± 41.66
1.27 ± 0.59	2.58 ± 2.88
4.63 ± 7.78	4.94 ± 11.68
12.70 ± 23.56	5.21 ± 18.19
3.68 ± 5.24	1.28 ± 2.03
9.79 ± 5.79	27.94 ± 99.29
8.09 ± 6.78	110.55 ± 536.76
0.09 ± 0.06	0.68 ± 2.09

Figure 4 Fold change between discrete liver statuses of normalized gene of interest expression in adipose, from ACTB expression, for Mean$\Delta\Delta Ct_{NAFLD}$/Mean$\Delta\Delta Ct_{Non\ NAFLD}$. Statistically significant values ($p<0.05$) are indicated (*). Non graphical display of means and standard deviations (SD) for non NAFLD and NAFLD (non NASH).

A trend for an increase in the expression of mRNAs encoding for lymphocyte differentiation transcription factors was observed in patients with NAFLD. This trend remained non-significant. For adipose expression levels of mRNA encoding *KCNRGv2*, a significant decrease was observed in those with NAFLD as compared to those classified as non NAFLD liver disease (Fold change = -2.30, $p<4.6e^{-02}$) (Figure 4).

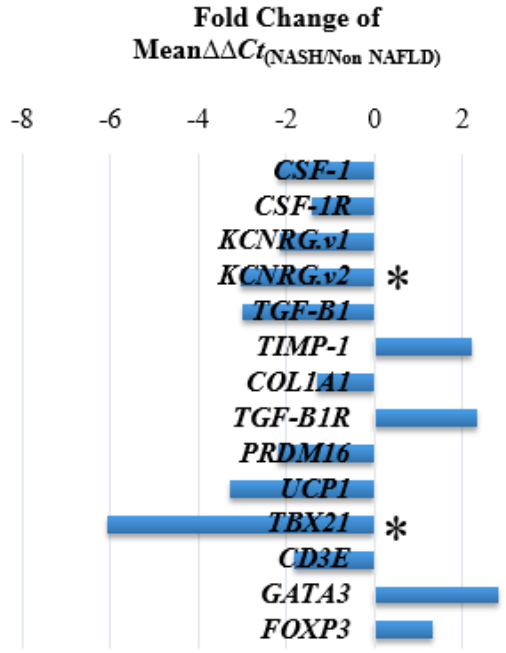

Non-NAFLD n= 11	NASH n= 91
Mean ± SD	Mean ± SD
2.28 ± 2.29	1.03 ± 1.46
20.85 ± 9.53	14.55 ± 8.00
1.20 ± 1.59	0.56 ± 0.60
0.30 ± 0.37	0.10 ± 0.24
0.17 ± 0.13	0.06 ± 0.07
63.86 ± 65.14	141.95 ± 118.94
81.53 ± 44.43	62.60 ± 66.02
1.27 ± 0.59	2.96 ± 3.72
4.63 ± 7.78	2.11 ± 4.22
12.70 ± 23.56	3.86 ± 6.12
3.68 ± 5.24	0.61 ± 0.51
9.79 ± 5.79	5.30 ± 5.59
8.09 ± 6.78	22.75 ± 67.77
0.09 ± 0.06	0.12 ± 0.15

Figure 5 Fold change between discrete liver statuses of normalized gene of interest expression in adipose, from ACTB expression, for Mean$\Delta\Delta Ct_{NASH}$/Mean$\Delta\Delta Ct_{Non\ NAFLD}$. Statistically significant values ($p<0.05$) are indicated (*). Non graphical display of means and standard deviations (SD) for non NAFLD and NASH.

When adipose samples collected from patients with NASH were compared to that of "non-NAFLD liver disease" patients, the expression levels of mRNAs encoding *KCNRGv2* (Fold change = -3.06, $p<1.2e^{-02}$) and *TBX21* (Fold change = -6.08, $p<4.9e^{-02}$) were found to be significantly down-regulated in NASH (Figure 5).

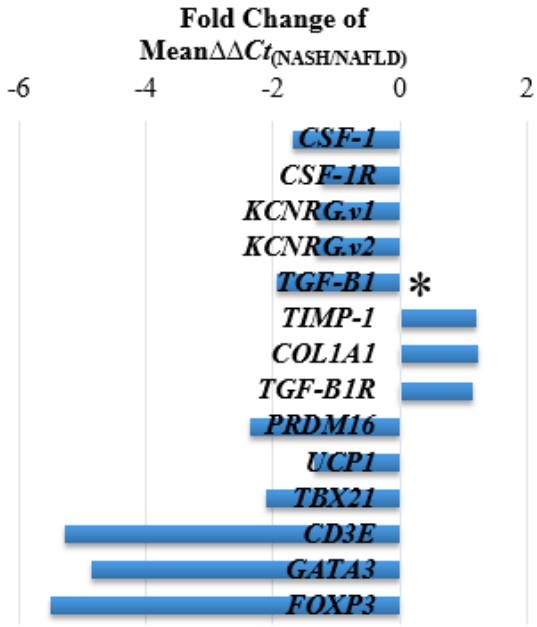

NAFLD n= 79	NASH n= 91
Mean ± SD	Mean ± SD
1.73 ± 2.65	1.03 ± 1.46
18.02 ± 13.53	14.55 ± 8.00
0.73 ± 0.74	0.56 ± 0.60
0.13 ± 0.24	0.10 ± 0.24
0.11 ± 0.17	0.06 ± 0.07
118.08 ± 134.66	141.95 ± 118.94
50.66 ± 41.66	62.60 ± 66.02
2.58 ± 2.88	2.96 ± 3.72
4.94 ± 11.68	2.11 ± 4.22
5.21 ± 18.19	3.86 ± 6.12
1.28 ± 2.03	0.61 ± 0.51
27.94 ± 99.29	5.30 ± 5.59
110.55 ± 536.76	22.75 ± 67.77
0.68 ± 2.09	0.12 ± 0.15

Figure 6 Fold change between discrete liver statuses of normalized gene of interest expression in adipose, from ACTB expression, for Mean$\Delta\Delta Ct_{NASH}$/Mean$\Delta\Delta Ct_{NAFLD}$. Statistically significant values ($p<0.05$) are indicated (*). Non graphical display of means and standard deviations (SD) for NAFLD (non NASH) and NASH .

In comparison of NASH and "non-NASH NAFLD" patients, an increase in the expression of *TIMP-1*, *COL1A1*, and *TGF-β1R* encoding mRNAs was noted in the NASH group. Simultaneously, a visible trend for decrease in levels of mRNAs encoding for T-lymphocyte transcription factors was detected. Yet, the only change in expression that reached significance was the down-regulation of *TGF-β1* (Fold change = -1.95, $p<4.0e^{-02}$) that was observed in the adipose tissue samples collected from patients with NASH as compared to those with non-NASH histological types of NAFLD (Figure 6).

For the following results the total cohort was used to analyze correlative relationships among the variables. A table of the means and standard deviations for each factor is included below (Table 4).

Table 4 Mean and standard deviation of variables assessed in this study.

Variable	N	Mean +/- Standard Deviation
Glucose (mg/dL)	223	107.27 +/- 36.69
HDL (mg/dL)	174	45.91 +/- 13.17
CSF-1 (AU)	84	1.51 +/- 2.13
CSF-1R (AU)	84	15.66 +/- 11.31
KCNRG v1 (AU)	82	0.70 +/- 0.73
KCNRG v2 (AU)	84	0.11 +/- 0.22
TGF-β1 (AU)	82	0.11 +/- 0.16
TIMP1 (AU)	83	126.97 +/- 161.12
COL1A1 (AU)	82	52.86 +/- 44.59
TGF-β1R (AU)	82	2.40 +/- 2.48
PRDM16 (AU)	81	3.25 +/- 6.69
UCP1 (AU)	82	9.23 +/- 24.11
TBX21 (AU)	79	0.89 +/- 1.30
CD3e (AU)	81	8.31 +/- 12.21
GATA3 (AU)	81	12.56 +/- 43.59
FOXP3 (AU)	80	0.20 +/- 0.46
Serum IL-1β (pg/mL)	234	2.22 +/- 0.65
Serum IL-2 (pg/mL)	236	2.16 +/- 12.35
Serum IL-4 (pg/mL)	235	1.46 +/- 1.04
Serum IL-5 (pg/mL)	234	2.19 +/- 1.81
Serum IL-6 (pg/mL)	235	8.89 +/- 10.45
Serum IL-7 (pg/mL)	234	11.18 +/- 5.23
Serum IL-8 (pg/mL)	236	19.49 +/- 22.86
Serum IL-10 (pg/mL)	234	4.07 +/- 13.30
Serum IL-12 (pg/mL)	236	23.16 +/- 43.97
Serum IL-13 (pg/mL)	235	2.78 +/- 2.82
Serum IL-17 (pg/mL)	235	7.73 +/- 17.20
Serum G-CSF (pg/mL)	236	8.87 +/- 13.75
Serum GM-CSF (pg/mL)	235	5.24 +/- 14.09
Serum IFN-γ (pg/mL)	236	47.94 +/- 81.07
Serum MCP-1(MCAF) (pg/mL)	235	72.80 +/- 44.63
Serum MIP-1β (pg/mL)	233	241.68 +/- 106.05
Serum TNF-α (pg/mL)	236	14.28 +/- 17.97
Serum TGF-β1 (pg/mL)	241	39125.55 +/- 43185.04

Table 5 Spearman's correlation analysis of expression levels of BMI, Glucose, and HDL with the levels of cytokines and inflammatory markers. NS stands for not significant (p-values are in parentheses). N=241.

	BMI	Glucose	HDL
BMI	1 (0)		
Serum Glucose (mg/dL)	NS	1 (0)	
Serum HDL (mg/dL)	NS	-0.28 ($p<2.4e^{-04}$)	1 (0)
***TGF-β1* (AU)**	NS	NS	0.34 ($p<4.4e^{-03}$)
Serum IL-4 (pg/mL)	-0.16 ($p <1.4e^{-02}$)	0.14 ($p<3.4e^{-02}$)	NS
Serum IL-5 (pg/mL)	NS	0.15 ($p<2.3e^{-02}$)	NS
Serum IL-6 (pg/mL)	0.28($p<1.9e^{-05}$)	NS	NS
Serum IL-8 (pg/mL)	-0.15 ($p<1.9e^{-02}$)	0.15 ($p<3.1e^{-02}$)	NS
Serum IL-10 (pg/mL)	NS	0.14 ($p<4.5e^{-02}$)	NS
Serum IL-17 (pg/mL)	-0.19 ($p<3.3e^{-03}$)	NS	NS
Serum G-CSF (pg/mL)	NS	0.15 ($p<2.3e^{-02}$)	NS
Serum TGF-β1 (pg/mL)	0.13 ($p<4.5e^{-02}$)	NS	NS
Ballooning Score	NS	0.19 ($p<6.0e^{-03}$)	-0.24 ($p<1.7e^{-03}$)
Bridging Fibrosis	NS	0.20 ($p<3.2e^{-03}$)	-0.17 ($p<2.8e^{-02}$)
Kupffer Cell Inflammation Score	NS	NS	-0.21 ($p<5.6e^{-03}$)
Lymphocyte Inflammation Score	NS	NS	-0.25 ($p<9.1e^{-04}$)
PMN InflammationScore	-0.14 ($p<3.0e^{-02}$)	0.14 ($p<3.8e^{-02}$)	-0.20 ($p<1.0e^{-02}$)
Mallory-Denk Score	NS	NS	-0.23 ($p<3.0e^{-03}$)
Pericellular Fibrosis Score	NS	0.14 ($p<3.8e^{-02}$)	-0.23 ($p<3.1e^{-03}$)
Portal Fibrosis Score	0.17 ($p<1.2e^{-02}$)	NS	NS
Portal Inflammation Score	NS	NS	-0.18 ($p<1.9e^{-02}$)
Diabetes Medication/Non-insulin	NS	0.40 ($p<5.8e^{-10}$)	NS
Hypertension Medication	0.13 ($p<4.7e^{-02}$)	0.24 ($p<5.7e^{-04}$)	NS
Hyperlipidemia Medication	NS	0.17 ($p<1.3e^{-02}$)	NS
Diabetes	NS	0.47 ($p<1.5e^{-13}$)	-0.18 ($p<2.0e^{-02}$)
Gender (Female)	-0.14 ($p<2.6e^{-02}$)	-0.17 ($p<1.3e^{-02}$)	0.28 ($p<1.7e^{-04}$)
Hypertension	NS	0.27 ($p<5.5e^{-05}$)	NS

Table 5 lists the variables that were found to positively or negatively correlate with BMI and the levels of glucose and high-density lipoprotein (HDL) in the blood.

Correlation coefficients rho (r) help to assess the strength of the linear relationship between two variables, while the coefficient of determination (r^2) measures

the accountability or how much of variable *y* can explain variable *x* (Taylor, 1990). Thus, our data may be interpreted as follows: BMI accounts for 3% of portal fibrosis ($r^2 = 0.03$) within this cohort of study and glucose levels in the blood accounts for 7% of incidence of hypertension ($r^2 = 0.07$).

In the entire cohort, BMI positively correlated with serum levels of IL-6 (r= 0.28, $p<1.9e^{-05}$) and TGF-β1 (r= 0.13, $p<4.5e^{-02}$), portal fibrosis (r= 0.17, $p<1.2e^{-02}$), and current use of hypertension medications (r=0.13, $p<4.7e^{-02}$). BMI negatively correlated with serum levels of IL-4 (r= -0.16, $p<1.4e^{-02}$), IL-8 (r=-0.15, $p<1.9e^{-02}$), IL-17 (r= -0.19, $p<3.3e^{-03}$), polymorphonuclear neutrophils infiltration in the liver (r= -0.14, $p<3.0e^{-02}$), and the female gender (r= -0.14, $p<2.6e^{-02}$). Glucose levels were positively correlated to the use of hypertension medication (r= 0.24, $p<5.7e^{-04}$) and diagnosis of hypertension (r= 0.27, $p<5.5e^{-05}$). Glucose levels inversely correlated with levels of HDL (r= -0.28, $p<2.4e^{-04}$). Positive correlations were observed between glucose levels and diagnosis of diabetes (r= 0.47, $p<1.5e^{-13}$) and use of non-insulin diabetic prescriptions (r= 0.40, $p<5.8e^{-10}$).

The levels of HDL, commonly known as “good” cholesterol, were inversely correlated with all types of scores for liver inflammation and fibrosis. A strong positive correlation was seen between levels of HDL and expression of mRNA encoding for *TGF-β1* in the visceral adipose tissue (r= 0.34, $p<4.4e^{-03}$).

Table 6 Spearman's correlation analysis of expression levels of mRNAs encoding *CSF-1, CSF-1R, KCNRGv1,* and *KCNRGv2* with inflammatory markers and cytokines (p-values are indicated in parentheses). N=241.

	CSF-1	***CSF-1R***	***KCNRG v1***	***KCNRG v2***
***CSF-1* (AU)**	1 (0)			
***CSF-1R* (AU)**	0.49 ($p<2.8e^{-06}$)	1 (0)		
***KCNRG v1* (AU)**	0.23 ($p<3.7e^{-02}$)	0.23 ($p<3.6e^{-02}$)	1 (0)	
***KCNRG v2* (AU)**	NS	NS	NS	1 (0)
***TGF-B1* (AU)**	0.29 ($p<9.7e^{-03}$)	NS	0.27 ($p<1.3e^{-02}$)	0.48 ($p<5.4e^{-06}$)
***TIMP-1* (AU)**	-0.29 ($p<8.0e^{-03}$)	NS	NS	NS
***TGF-B1R* (AU)**	NS	NS	0.27 ($p<1.5e^{-02}$)	NS
***PRDM16* (AU)**	0.36 ($p<9.6e^{-04}$)	NS	NS	0.29 ($p<9.2e^{-03}$)
***UCP1* (AU)**	0.24 ($p<3.5e^{-02}$)	NS	NS	0.26 ($p<2.0e^{-02}$)
***TBX21* (AU)**	NS	NS	NS	0.22 ($p<4.9e^{-02}$)
***CD3E* (AU)**	NS	NS	NS	0.26 ($p<2.1e^{-02}$)
Serum IL-4 (pg/mL)	-0.26 ($p<2.2e^{-02}$)	NS	NS	NS
Serum IL-5 (pg/mL)	-0.33 ($p<2.5e^{-03}$)	NS	NS	-0.25 ($p<2.4e^{-02}$)
Serum IL-12 (pg/mL)	NS	-0.25 ($p<2.4e^{-02}$)	NS	NS
Serum IL-13 (pg/mL)	-0.30 ($p<7.9e^{-03}$)	NS	NS	NS
Serum IL-17 (pg/mL)	-0.25 ($p<2.8e^{-02}$)	NS	NS	NS
Serum IFN-γ (pg/mL)	NS	-0.25 ($p<2.5e^{-02}$)	NS	NS
Serum TNF-α (pg/mL)	NS	NS	NS	-0.25 ($p<2.5e^{-02}$)
Kupffer Cell Inflammation Score	-0.23 ($p<3.6e^{-02}$)	NS	NS	-0.34 ($p<2.1e^{-03}$)
PMN Inflammation Score	NS	NS	NS	-0.39 ($p<2.8e^{-04}$)
Portal Fibrosis Score	-0.22 ($p<4.4e^{-02}$)	NS	NS	NS
Portal Inflammation Score	-0.23 ($p<4.0e^{-02}$)	NS	NS	NS
Hypertension Medication	-0.36 ($p<9.9e^{-04}$)	NS	NS	NS
Hypertension	-0.33 ($p<3.2e^{-03}$)	NS	NS	NS

The correlation analysis of expression levels of mRNAs encoding for *CSF-1*, *CSF-1R, KCNRGv1*, and *KCNRGv2* revealed many significant trends (Table 6). In visceral adipose samples, the levels of mRNA encoding for *CSF-1* were positively correlated with that of mRNA encoding for *CSF-1R* (r= 0.49, $p<2.8e^{-06}$) and notably also with that of mRNA encoding for *PRDM16* (r= 0.36, $p<9.6e^{-04}$). Additionally, the levels of mRNA encoding for CSF-1 were inversely correlated with serum levels of IL-5 (r= -

0.33, $p<2.5e^{-03}$), the presence of hypertension (r= -0.33, $p<3.2e^{-03}$), and use of anti-hypertension medication (r= -0.36, $p<9.9e^{-04}$). Our data show that mRNA levels of *CSF-1* in adipose accounts for the 11% of the decrease in serum levels of IL-5 ($r^2 = 0.11$), and possibly influencing differentiation of BAT as the expression levels of *CSF-1* explains 13% of *PRDM16* expression ($r^2 = 0.13$).

The expression levels of mRNAs encoding for *CSF-1R* and *KCNRGv1* demonstrated a few weak correlations, namely, the levels of *CSF-1R* encoding mRNA were positively correlated with mRNA expression levels of *KCNRGv1* (r= 0.23, $p<3.6e^{-02}$) and negatively with serum levels of IL-12 (r= -0.25, $p<2.4e^{-02}$) and IFN-γ (r= -0.25, $p<2.5e^{-02}$). In adipose samples, the expression levels of mRNA encoding for *KCNRGv1* were positively correlated with that of *TGF-β1* (r= 0.27, $p<1.3e^{-02}$) and its receptor *TGF-β1R* (r= 0.27, $p<1.5e^{-02}$).

Interestingly, in our study, the mRNA levels of *KCNRGv2* expression accounted for 23% of *TGF-β1* mRNA expression in adipose ($r^2 = 0.23$), while being inversely correlated with presence of Kupffer cells and PMN (polymorphonuclear neutrophils) inflammation in the liver.

Table 7 Spearman's correlation of *TGF-β1, TIMP-1, COL1A1, TGF-β1R* with inflammatory markers and cytokines (p-values are indicated in parentheses). N=241.

	TGF-B1	***TIMP-1***	***COL1A1***	***TGF-B1R***
***TGF-B1* (AU)**	1 (0)			
***TIMP-1* (AU)**	NS	1 (0)		
***COL1A1* (AU)**	NS	NS	1 (0)	
***TGF-B1R* (AU)**	NS	NS	NS	1 (0)
***PRDM16* (AU)**	0.43 ($p<7.6e^{-05}$)	-0.2 ($p<2.5e^{-02}$)	NS	NS
***UCP1* (AU)**	0.35 ($p<1.4e^{-03}$)	NS	NS	0.29 ($p<9.5e^{-03}$)
***TBX21* (AU)**	NS	NS	NS	0.36 ($p<1.3e^{-03}$)
***CD3E* (AU)**	0.39 ($p<4.0e^{-04}$)	NS	NS	0.40 ($p<2.3e^{-04}$)
***FOXP3* (AU)**	0.42 ($p<1.2e^{-04}$)	NS	NS	NS
Serum IL-1β (pg/mL)	-0.31 ($p<6.8e^{-03}$)	NS	NS	NS
Serum IL-4 (pg/mL)	-0.23 ($p<4.1e^{-02}$)	NS	NS	NS
Serum IL-6 (pg/mL)	-0.28 ($p<1.3e^{-02}$)	NS	NS	NS
Serum IL-13 (pg/mL)	-0.30 ($p<7.6e^{-03}$)	NS	NS	NS
Ballooning Score	-0.22 ($p<4.4e^{-02}$)	NS	NS	NS
Kupffer Cell Inflammation Score	-0.37 ($p<7.1e^{-04}$)	NS	NS	NS
Lymphocyte Inflammation Score	-0.34 ($p<2.1e^{-03}$)	NS	NS	NS
PMN Inflammation Score	-0.28 ($p<1.0e^{-02}$)	0.29 ($p<8.0e^{-03}$)	NS	NS
Pericellular Fibrosis Score	NS	0.26 ($p<1.8e^{-02}$)	NS	NS
Hypertension Medication	NS	NS	-0.30 ($p<6.8e^{-03}$)	NS
Diabetes	NS	0.23 ($p<4.0e^{-02}$)	NS	NS
Gender (Female)	0.28 ($p<1.0e^{-02}$)	NS	NS	NS
Hypertension	NS	NS	-0.30 ($6.9e^{-03}$)	NS

In analysis of correlations of the levels of mRNAs encoding for *TGF-β1*, *TIMP-1*, *COL1A1*, and *TGF-β1R* (Table 7), the levels of mRNA encoding for *TGF-β1* were positively correlated with that for *PRDM16* (r= 0.43, $p<7.6e^{-05}$), *UCP1* (r= 0.35, $p<1.4e^{-03}$), *CD3E* (r= 0.39, $p<4.0e^{-04}$), and *FOXP3* (r= 0.42, $p<1.2e^{-04}$). In adipose tissue, the levels of mRNA encoding for *TGF-β1* were inversely correlated to serum levels of IL-1β (r= -0.31, $p<6.8e^{-03}$) and IL-13 (r= -0.30, $p<7.6e^{-03}$), number of Kupffer cells (r= -0.37,

$p<7.1e^{-04}$), and scores for lymphocyte infiltration (r= -0.34, $p<2.1e^{-03}$); hence, the trends were the same as shown earlier (Table 5 and 6).

In visceral adipose, the levels of mRNA encoding for *TIMP-1* were positively correlated to the occurrence of diabetes (r= 0.23, $p<4.0e^{-02}$). It was suggested that levels of angiogenesis inhibitor *TIMP-1* may contribute to the poor blood circulation commonly seen in patients with type II diabetes. The levels of mRNA encoding for *COL1A1*were correlated with use of hypertension medication (r= -0.30, $p<6.8e^{-03}$) and the presence of hypertension (r= -0.30, $p<6.9e^{-03}$), while the levels of mRNA encoding for *TGF-β1R* were positively correlated with that of *TBX21* (r= 0.36, $p<1.3e^{-03}$) and *CD3E* (r= 0.40, $p<2.3e^{-04}$).

Table 8 Spearman's correlation analysis of expression levels of mRNAs encoding *PRDM16, UCP1, TBX21, and CD3E* with inflammatory markers and cytokines (p-values are indicated in parentheses). N=241

	PRDM16	***UCP1***	***TBX21***	***CD3E***
***PRDM16* (AU)**	1 (0)			
***UCP1* (AU)**	0.60 ($p<4.0e^{-09}$)	1 (0)		
***TBX21* (AU)**	NS	0.23 ($p<4.2e^{-02}$)	1 (0)	
***CD3E* (AU)**	0.36 ($p<1.3e^{-03}$)	0.27 ($p<1.6e^{-02}$)	0.62 ($p<1.4e^{-09}$)	1 (0)
***GATA3* (AU)**	NS	0.23 ($p<4.4e^{-02}$)	0.32 ($p<3.8e^{-03}$)	NS
***FOXP3* (AU)**	NS	NS	0.28 ($p<1.4e^{-02}$)	0.36 ($p<1.1e^{-03}$)
Serum IL-12 (pg/mL)	NS	NS	0.24 ($p<3.6e^{-02}$)	NS
Lymphocyte Inflammation Score	-0.28 ($p<1.2e^{-02}$)	-0.33 ($p<2.8e^{-03}$)	NS	NS
Gender (Female)	NS	0.34 ($p<1.6e^{-03}$)	NS	NS

An analysis of correlations for the BAT and immune cell biomarker molecules *PRDM16, UCP1, TBX21*, and *CD3E* presented in Table 8. The positive correlation between expression levels of mRNA encoding for *PRDM16* and *UCP1* (r= 0.60, $p<4.0e^{-}$

^{09}) is not surprising, as *PRDM16* is a known regulator of *UCP1* expression (Seale P et al., 2007). Interestingly, expression levels of mRNA encoding for *UCP1* were inversely correlated with lymphocyte infiltration (r= -0.33, $p<2.8e^{-03}$), while being positively associated with female gender (r= 0.34, $p<1.6e^{-03}$).

The expression levels for T-lymphocyte transcription factor encoding mRNAs *TBX21* and *CD3E* (r= 0.62, $p<1.4e^{-09}$) correlated with each other. A similar positive correlation was also seen for the expression levels of *FOXP3* and *CD3E* encoding mRNAs (r= 0.36, $p<1.1e^{-03}$).

Table 9 Spearman's correlation analysis of expression levels of mRNAs encoding *GATA3, FOXP3* and serum levels of IL-1β and IL-2 with inflammatory markers and cytokines (p-values are indicated in parentheses). N=241.

	GATA3	***FOXP3***	**Serum IL-1β**	**Serum IL-2**

***GATA3* (AU)**	1 (0)			
***FOXP3* (AU)**	NS	1 (0)		
Serum IL-1β (pg/mL)	NS	NS	1 (0)	
Serum IL-2 (pg/mL)	NS	NS	0.17 ($p<1.1e^{-02}$)	1 (0)
Serum IL-4 (pg/mL)	NS	-0.28 ($p<1.4e^{-02}$)	0.70 ($p<1.9e^{-35}$)	NS
Serum IL-5 (pg/mL)	NS	NS	0.28 ($p<1.2e^{-05}$)	NS
Serum IL-6 (pg/mL)	NS	NS	0.45 ($p<4.2e^{-13}$)	0.41 ($p<8.6e^{-11}$)
Serum IL-7 (pg/mL)	NS	NS	0.52 ($p<3.4e^{-17}$)	0.13 ($p<4.2e^{-02}$)
Serum IL-8 (pg/mL)	NS	NS	0.41 ($p<5.6e^{-11}$)	NS
Serum IL-10 (pg/mL)	NS	NS	0.25 ($p<1.0e^{-04}$)	0.25 ($p<1.1e^{-04}$)
Serum IL-12 (pg/mL)	NS	NS	0.47 ($p<5.7e^{-14}$)	0.19 ($p<3.5\ e^{-03}$)
Serum IL-13 (pg/mL)	NS	NS	0.71 ($p<2.1e^{-36}$)	0.26 ($p<4.0e^{-05}$)
Serum IL-17 (pg/mL)	NS	NS	0.23 ($p<3.6e^{-04}$)	NS
Serum G-CSF (pg/mL)	NS	NS	0.57 ($p<1.9e^{-21}$)	NS
Serum GM-CSF (pg/mL)	NS	NS	0.13 ($p<4.7e^{-02}$)	0.29 ($p<5.2e^{-06}$)
Serum IFN-γ (pg/mL)	NS	NS	0.63 ($p<1.5e^{-27}$)	0.15 ($p<2.0e^{-02}$)
Serum MCP-1(MCAF) (pg/mL)	NS	NS	0.15 ($p<1.9e^{-02}$)	0.27 ($p<2.6e^{-05}$)
Serum MIP-1b (pg/mL)	NS	NS	0.30 ($p<3.7e^{-06}$)	0.24 ($p<2.6e^{-04}$)
Serum TNF-α (pg/mL)	NS	NS	0.59 ($p<3.8e^{-23}$)	0.13 ($p<5.0e^{-02}$)
Bridging Score	NS	-0.22 ($p<4.8e^{-02}$)	NS	NS
Kupffer Cell Inflammation Score	NS	NS	0.16 ($p<1.6e^{-02}$)	NS
Mallory-Denk Score	-0.24 ($p<3.0e^{-02}$)	-0.29 ($p<8.6e^{-03}$)	NS	NS
Gender (Female)	NS	0.24 ($p<3.5e^{-02}$)	NS	NS

The results of the correlation analysis for adipose expression levels of mRNAs encoding for *GATA3* and *FOXP3*, and serum levels of cytokines IL-1β and IL-2 are presented in Table 9. Adipose expression levels of mRNAs encoding for GATA3 and FOXP3 were inversely correlated with inflammatory markers, including Mallory-Denk bodies ($r= -0.24$, $p<3.0e^{-02}$) and infiltration scores ($r= -0.29$, $p<8.6e^{-03}$). Expression levels

of mRNAs encoding for FOXP3 was inversely correlated with serum levels of IL-4 (r= -0.28, $p<1.4e^{-02}$).

Serum levels of IL-1β were positive correlated with that of IL-4 (r= 0.70, $p<1.9e^{-35}$), as well as IL-13 (r= 0.71, $p<2.1e^{-36}$) and IFN-γ (r= 0.63, $p<1.5e^{-27}$). Serum levels of IL-2 were positive correlated with inflammatory cytokine IL-6 (r= 0.41, $p<8.6e^{-11}$).

The correlations of the levels of IL-4, IL-5, IL-6, and IL-7 in the serum are shown in Table 10. Serum levels of IL-4 were positively correlated with that of IL-5 (r= 0.67, $p<1.6e^{-31}$), G-CSF (r= 0.62, $p<1.6e^{-26}$), and TNF-α (r= 0.74, $p<2.3e^{-42}$). The levels of IL-5 were positively correlated with that of TNF-α (r= 0.71, $p<4.6e^{-37}$) and IL-17 (r= 0.72, $p<6.1e^{-39}$). The serum levels of IL-6 demonstrated positive correlations with that of IL-12 (r= 0.44, $p<1.8e^{-12}$) and INF-γ (r= 0.45, $p<4.7e^{-13}$), while the levels of IL-7 were positively correlated with that of IL-8 (r= 0.45, $p<7.6e^{-13}$), IL-12 (r= 0.45, $p<5.1e^{-13}$), IL-13 (r= 0.46, $p<1.1e^{-13}$), INF-γ (r= 0.48, $p<3.9e^{-15}$), G-CSF (r= 0.42, $p<2.6e^{-11}$), and TNF-α (r= 0.42, $p<3.3e^{-11}$).

Table 10 Spearman's correlation analysis of serum levels of IL-4, IL-5, IL-6, and IL-7 with inflammatory markers and cytokines (p-values are indicated in parentheses). N=241.

	Serum IL-4	Serum IL-5	Serum IL-6	Serum IL-7
Serum IL-4 (pg/mL)	1 (0)			

Serum IL-5 (pg/mL)	0.67 ($p<1.6e^{-31}$)	1 (0)		
Serum IL-6 (pg/mL)	0.30 ($p<2.5e^{-06}$)	NS	1 (0)	
Serum IL-7 (pg/mL)	0.47 ($p<5.6e^{-14}$)	0.40 ($p<2.5e^{-10}$)	0.34 ($p<1.1e^{-07}$)	1 (0)
Serum IL-8 (pg/mL)	0.58 ($p<1.9e^{-22}$)	0.55 ($p<1.3e^{-19}$)	0.39 ($p<6.3e^{-10}$)	0.45 ($p<7.6e^{-13}$)
Serum IL-10 (pg/mL)	0.38 ($p<1.8e^{-09}$)	0.50 ($p<9.1e^{-16}$)	0.30 ($p<3.0e^{-06}$)	0.40 ($p<4.2e^{-10}$)
Serum IL-12 (pg/mL)	0.56 ($p<1.5e^{-20}$)	0.50 ($p<2.7e^{-16}$)	0.44 ($p<1.8e^{-12}$)	0.45 ($p<5.1e^{-13}$)
Serum IL-13 (pg/mL)	0.60 ($p<5.0e^{-24}$)	0.31 ($p<1.3e^{-06}$)	0.37 ($p<3.4e^{-09}$)	0.46 ($p<1.1e^{-13}$)
Serum IL-17 (pg/mL)	0.56 ($p<9.8e^{-21}$)	0.72 ($p<6.1e^{-39}$)	NS	0.22 ($p<6.2e^{-04}$)
Serum G-CSF (pg/mL)	0.62 ($p<1.6e^{-26}$)	0.40 ($p<2.3e^{-10}$)	0.28 ($p<1.4e^{-05}$)	0.42 ($p<2.6e^{-11}$)
Serum GM-CSF (pg/mL)	NS	NS	NS	0.17 ($p<9.7e^{-03}$)
Serum IFN-γ (pg/mL)	0.59 ($p<5.2e^{-23}$)	0.42 ($p<1.5e^{-11}$)	0.45 ($p<4.7e^{-13}$)	0.48 ($p<3.9e^{-15}$)
Serum MCP-1(MCAF) (pg/mL)	NS	NS	0.32 ($p<8.3e^{-07}$)	0.30 ($p<2.4e^{-06}$)
Serum MIP-1b (pg/mL)	0.27 ($p<4.4e^{-05}$)	NS	0.32 ($p<5.7e^{-07}$)	0.31 ($p<1.5e^{-06}$)
Serum TNF-α (pg/mL)	0.74 ($p<2.3e^{-42}$)	0.71 ($p<4.6e^{-37}$)	0.30 ($p<3.4e^{-06}$)	0.42 ($p<3.3e^{-11}$)
Serum TGF-β1 (pg/mL)	-0.18 ($p<7.0e^{-03}$)	-0.48 ($p<8.0e^{-15}$)	NS	NS
Ballooning Score	NS	NS	0.17 ($p<1.0e^{-02}$)	NS
Bridging Score	NS	0.13 ($p<4.6e^{-02}$)	NS	NS
Kupffer Cell Inflammation Score	NS	NS	0.20 ($p<2.6e^{-03}$)	NS
PMN Inflammation Score	0.18 ($p<7.2e^{-03}$)	0.23 ($p<4.5e^{-04}$)	NS	NS
Mallory-Denk Score	NS	0.19 ($p<3.8e^{-03}$)	NS	NS
Pericellular Fibrosis Score	0.15 ($p<2.4e^{-02}$)	0.25 ($p<1.5e^{-04}$)	NS	NS
Portal Fibrosis Score	NS	0.18 ($p<7.6e^{-03}$)	0.14 ($p<3.7e^{-02}$)	NS
Portal Inflammation Score	NS	NS	0.18 ($p<7.4e^{-03}$)	NS
Diabetes Med./Non-insulin	NS	0.19 ($p4.2e^{-03}$)	NS	NS
Diabetes	NS	0.25 ($p<1.1e^{-04}$)	NS	NS

Table 11 Spearman's correlation analysis of serum levels of IL-8, IL-10, IL-12, and IL-13 with inflammatory markers and cytokines (p-values are indicated in parentheses). N=241.

	Serum IL-8	**Serum IL-10**	**Serum IL-12**	**Serum IL-13**
Serum IL-8 (pg/mL)	1 (0)			

Serum IL-10 (pg/mL)	0.42 ($p<3.9e^{-11}$)	1 (0)		
Serum IL-12 (pg/mL)	0.38 ($p<1.4e^{-09}$)	0.43 ($p<3.3e^{-12}$)	1 (0)	
Serum IL-13 (pg/mL)	0.44 ($p<3.3e^{-12}$)	0.34 ($p<1.5e^{-07}$)	0.55 ($p<3.4e^{-20}$)	1 (0)
Serum IL-17 (pg/mL)	0.46 ($p<8.0e^{-14}$)	0.41 ($p<5.7e^{-11}$)	0.25 ($p<1.4e^{-04}$)	0.33 ($p<3.9e^{-07}$)
Serum G-CSF (pg/mL)	0.41 ($p<1.1e^{-10}$)	0.28 ($p<1.2e^{-05}$)	0.33 ($p<1.6e^{-07}$)	0.47 $p<5.0e^{-14}$)
Serum GM-CSF (pg/mL)	NS	0.23 ($p<3.3e^{-04}$)	NS	NS
Serum IFN-γ (pg/mL)	0.33 ($p<3.6e^{-07}$)	0.30 ($p<3.3e^{-06}$)	0.71 ($p<3.0e^{-37}$)	0.42 ($p<2.1e^{-11}$)
Serum MCP-1(MCAF) (pg/mL)	0.16 ($p<1.5e^{-02}$)	NS	NS	0.14 ($p<3.7e^{-02}$)
Serum MIP-1b (pg/mL)	0.39 ($p<8.6e^{-10}$)	0.17 ($p<9.0e^{-03}$)	0.14 ($p<3.4e^{-02}$)	0.32 ($p<5.3e^{-07}$)
Serum TNF-α (pg/mL)	0.50 ($p<3.1e^{-16}$)	0.40 ($p<3.2e^{-10}$)	0.60 ($p<2.6e^{-23}$)	0.46 ($p<1.1e^{-13}$)
Serum TGF-β1 (pg/mL)	-0.24 ($p<1.5e^{-04}$)	-0.23 ($p<3.5e^{-04}$)	-0.15 ($p<2.4e^{-02}$)	NS
Ballooning Score	0.28 ($p<1.8e^{-05}$)	NS	NS	NS
Bridging Score	0.26 ($p<8.3e^{-05}$)	NS	NS	NS
Kupffer Cell Inflammation Score	0.23 ($p<6.2e^{-04}$)	NS	NS	0.19 ($p<4.2e^{-03}$)
Lymphocyte Inflammation Score	NS	NS	NS	0.14 ($p<3.1e^{-02}$)
PMN Inflammation Score	0.23 ($p<5.2e^{-04}$)	0.14 ($p<4.0e^{-02}$)	NS	NS
Mallory-Denk Score	0.29 ($p<8.7e^{-06}$)	NS	NS	NS
Pericellular Fibrosis Score	0.32 ($p<1.2e^{-06}$)	0.14 ($p<3.4e^{-02}$)	NS	0.14 ($p<3.2e^{-02}$)
Portal Fibrosis Score	0.21 ($p<1.6e^{-03}$)	NS	NS	NS
Portal Inflammation Score	0.20 ($p<2.1e^{-03}$)	NS	NS	NS
Diabetes Medication/Non-insulin	NS	0.14 ($p<3.2e^{-02}$)	NS	NS
Diabetes	0.14 ($p<3.3e^{-02}$)	0.20 ($p<2.8e^{-03}$)	NS	NS

Correlation analysis for serum levels of IL-8, IL-10, IL-12, and IL-13 revealed further complexity of their relationships to each other (Table 11). For example, the levels of IL-8 were positively correlated with that of IL-10 (r= 0.42, $p<3.9e^{-11}$), IL-13 (r= 0.44, $p<3.3e^{-12}$), IL-17 (r= 0.46, $p<8.0e^{-14}$), G-CSF (r= 0.41, $p<1.1e^{-10}$), and TNF-α (r= 0.50, $p<3.14e^{-16}$). The levels of IL-10 were correlated with that of IL-12 (r= 0.43, $p<3.332e^{-12}$)

and IL-17 (r= 0.41, $p<5.7e^{-11}$), while the levels of TNF-α (r= 0.59, $p<2.6e^{-23}$) and IL-13 (r= 0.55, $p<3.4e^{-20}$) were positively correlated with that of IL-12. The levels of IL-12 were strongly correlated with that of IFN-γ (r= 0.71, $p<3.0e^{-37}$). The levels of IL-13 were correlated with that of G-CSF (r= 0.47, $p<4.949e^{-14}$), IFN-γ (r= 0.42, $p<2.1e^{-11}$), and TNF-α (r= 0.46, $p<1.1e^{-13}$).

Table 12 Spearman's correlation analysis of serum levels of IL-17, G-CSF, GM-CSF, and IFN-γ with inflammatory markers and cytokines (p-values are indicated in parentheses). N=241.

	Serum IL-17	Serum G-CSF	Serum GM-CSF	Serum IFN-γ
Serum IL-17 (pg/mL)	1 (0)			
Serum G-CSF (pg/mL)	0.39 ($p<4.6e^{-10}$)	1 (0)		
Serum GM-CSF (pg/mL)	NS	0.19 ($p<4.5e^{-03}$)	1 (0)	
Serum IFN-γ (pg/mL)	NS	0.40 ($p<2.3e^{-10}$)	NS	1 (0)
Serum MCP-1(MCAF) (pg/mL)	NS	NS	0.18 ($p<7.3e^{-03}$)	NS
Serum MIP-1b (pg/mL)	0.20 ($p<2.8e^{-03}$)	0.22 ($p<6.5e^{-04}$)	NS	NS
Serum TNF-α (pg/mL)	0.48 ($p<4.7e^{-15}$)	0.47 ($p<2.1e^{-14}$)	NS	0.66 ($p<2.2e^{-30}$)
Serum TGF-β1 (pg/mL)	-0.44 ($p<9.8e^{-13}$)	NS	0.15 ($p<2.1e^{-02}$)	NS
Bridging Score	0.13 ($p<4.7e^{-02}$)	NS	NS	NS
Kupffer Cell Inflam Score	NS	NS	NS	0.14 ($p<3.0e^{-02}$)
Lymphocyte Inflam Score	0.16 ($p<1.3e^{-02}$)	NS	NS	NS
Mallory-Denk Score	0.14 ($p<3.8e^{-02}$)	NS	NS	NS
Pericellular Fib. Score	0.25 ($p<1.9e^{-04}$)	NS	NS	NS
Portal Fibrosis Score	0.14 ($p<3.9e^{-02}$)	NS	NS	NS
Diabetes Med/Non-insulin	NS	NS	NS	0.14 ($p<3.9e^{-02}$)

Significant correlations identified for serum levels of IL-17, G-CSF, GM-CSF, and IFN-γ are summarized in Table 12. The serum levels of IL-17 were positively correlated with that of G-CSF (r= 0.39, $p<4.6e^{-10}$) and TNF-α (r= 0.48, $p<4.7e^{-15}$), yet inversely correlated with serum levels of TGF-β1 (r= -0.44, p<9.8e-13). The levels of G-CSF were correlated to that of IFN-γ (r= 0.40, $p<2.3e^{-10}$) and TNF-α (r= 0.47, $p<2.1e^{-14}$).

Notably, serum levels of IFN-γ were strongly correlated with that of TNF-α (r= 0.66, $p<2.2e^{-30}$).

Table 13 Spearman's correlation analysis of serum levels of MCP-1, MIP-1b, TNF-α, and TGF-β1 with inflammatory markers and cytokines (p-values are indicated in parentheses). N=241.

	Serum MCP-1 (MCAF)	Serum MIP-1b	Serum TNF-α	Serum TGF-β1
Serum MCP-1 (MCAF) (pg/mL)	1 (0)			
Serum MIP-1b (pg/mL)	0.31 ($p<1.2e^{-06}$)	1 (0)		
Serum TNF-α (pg/mL)	NS	0.14 ($p<3.9e^{-02}$)	1 (0)	
Serum TGF-β1 (pg/mL)	NS	NS	-0.26 ($p<3.9e^{-05}$)	1 (0)
Ballooning Score	NS	0.15 ($p<2.7e^{-02}$)	NS	NS
Bridging Score	0.16 ($p<1.9e^{-02}$)	NS	NS	-0.15 ($p<2.7e^{-02}$)
Kupffer Cell Inflammation Score	NS	0.15 ($p<2.3e^{-02}$)	NS	NS
Lymphocyte Inflammation Score	0.16 ($p<1.9e^{-02}$)	NS	NS	NS
PMN Inflammation Score	NS	NS	0.16 ($p<1.5e^{-02}$)	-0.15 ($p<2.2e^{-02}$)
Mallory-Denk Score	NS	0.15 ($p<3.0e^{-02}$)	NS	-0.20 ($p<1.9e^{-03}$)
Pericellular Fibrosis Score	NS	0.21 ($p<1.7e^{-03}$)	NS	-0.26 ($p<5.3e^{-05}$)
Portal Fibrosis Score	0.14 ($p<3.0e^{-02}$)	NS	NS	-0.19 ($p<3.8e^{-03}$)
Portal Inflammation Score	0.15 ($p<2.3e^{-02}$)	NS	NS	NS
Diabetes Medication/Non-insulin	NS	NS	0.15 ($p<2.1e^{-02}$)	NS
Diabetes	NS	NS	0.13 ($p<3.9e^{-02}$)	NS

The results of correlation analysis for serum levels of MCP-1, MIP-1b, TNF-α, and TGF-β1 are presented in Table 13. Serum levels of MCP-1 were positively correlated to that of MIP-1b (r= 0.31, $p<1.2e^{-06}$). Notably, serum levels of TNF-α were inversely correlated to the levels of circulating TGF-β1 (r= -0.26, $p<3.9e^{-05}$) in the serum.

DISCUSSION

Adipose Tissue

Speaking generally, a majority of human organs are highly organized assemblies of phenotypically diverse cells that are known to closely interact with each other. In this regard, adipose tissue is no different. It is not only comprised of different types of adipocytes, such as white and brown, but also includes macrophages, lymphocytes and blood vessels comprising of endotheliocytes. All of these cells communicate through the release of various signaling molecules, which affect the immediate cells in the local environment and/or are carried systemically throughout the body by the blood.

These cytokines/adipokines can act either in a pro or anti-inflammatory manner. Many cytokines/adipokines originate in the adipose tissue and are carried throughout the body, thus, influencing the immune response and cell signaling in other tissues. Cytokines of adipose origin can preferentially act on organs that reside in close proximity to visceral fat depot, as in the case of the liver. Some signals also known to act locally, perpetuate the vicious cycle of inflammation within adipose tissue itself.

In this study, we profiled both the histological indicators of liver inflammation/fibrosis and the expression of pro-inflammatory molecules in visceral adipose. Our data provide evidence that adipose produces pro-inflammatory substances that influence both pro and anti-inflammatory pathways in other organs, particularly, in

the liver. We also provide evidence of existence of brown adipose cells scattered in the visceral adipose and their possibly involvement in an anti-inflammatory response.

Pro-inflammatory Mediators

As indicated by analysis of correlations for the histological scores for portal inflammation, lymphoplasmacytic lobular inflammation, polymorphonuclear lobular inflammation, Kupffer cell hypertrophy, apoptotic bodies, focal parenchymal necrosis, glycogen nuclei, hepatocellular ballooning, and Mallory-Denk bodies, the following molecules were identified as possible contributing factors to hepatic inflammation: an expression of mRNA encoding for *TIMP-1* in adipose, and serum levels of IL-1β, IL-4, IL-5, IL-6, IL-8, IL-10, IL-13, IL-17, IFN-γ, MCP-1, MIP-1b, and TNF-α.

There was no surprise that serum pro-inflammatory markers were positively correlated to both BMI and serum glucose levels. However, it is interesting to note that the use of hypertension treating medication was positively correlated with BMI, reflecting an increase in hypertension incidence with obesity. BMI itself was not correlated to the diagnosis of diabetes as one could expect, thus, stressing the possibility of so called "metabolically healthy" obesity phenotype, as that observed in *Brd2* knockout mice (Wang et al., 2013) and some humans (Stefan et al., 2013).

The positive correlations seen between glucose levels and presence of diabetes was expected since high glucose levels are part of the clinical definition of type II diabetes that results from an increase in insulin resistance preventing cells from taking in the excess of circulating glucose. Glucose levels were also inversely correlated with HDL levels.

As mentioned before, metalloproteinase inhibitor TIMP-1 is produced by macrophages, its local production usually indicates the infiltration of the tissue by of immune cells. In visceral adipose tissue, the production of TIMP-1 may aid in suppression of the new blood vessel formation. Thus, macrophage production of TIMP-1 may contribute to the poor circulation commonly observed in patients with obesity associated diabetes mellitus and may instigate the development of microangiopathy. However, it is still uncertain whether TIMP-1 is directly involved in the development of this condition. Further experimentation including the development of an animal model is needed to evaluate the validity of this hypothesis.

Notably, serum levels of a majority of the cytokines/interleukins profiled in this study were positively correlated with the histological scores of inflammation in respective liver biopsies. The serum levels of inflammatory marker IL-17 that is produced by mature Th17 cells (Harrington et al., 2005), was inversely correlated to that of IFN-γ. Interestingly, mature IL-17 cells are not inhibited by IFN-γ (Harrington et al., 2005), that is produced by Th1 cells and induces damage to tissues and macrophage cytokine production, while inhibiting Th2 cells proliferation.

IL-4, IL-5, IL-10, and IL-13 are cytokines released by Th2 cells and natural killer T-cells that also produce IL-13. The NAFLD-associated changes in the expression of genes encoding for transcription factors specifying the differentiation of T cells into Th1 or Th2 lineages indicate a shift in the patterns of T-helper cells. It has been previously shown that interfering with GATA3 entirely inhibits T-cell development, indicating its importance in thymocyte formation (Ting et al., 1996). The differences in expression of

GATA3 in adipose between liver disease states were not found to be significant; hence, the shift is not related to generation of T cells in general, but rather relates to T helper cells. Thus, our study supports the hypothesis that inflammation within visceral adipose is shaped by the regulation of the homeostasis of pro and anti-inflammatory immune cells that is skewed in obese individuals towards a more pro-inflammatory status.

TNF-α's role in cell apoptosis and inflammation is well studied. Here we found more evidence to back this claim. The levels of TNF-α in serum were not only correlated with levels of IFN-γ, but with that of many other pro-inflammatory cytokines, including IL-1β, IL-4, IL-5, IL-6, IL-8, IL-10, IL-12, IL-13, and IL-17. It seems like TNF-α may be a chief orchestrator in the activation of systemic background inflammation associated with obesity.

Anti-inflammatory Mediators

In adipose tissue, TGF-β1 is secreted predominantly by non-fat cells (Fain et al., 2005; Wahl et al., 1990). We observed that a decrease in the expression of mRNA encoding for *TGF-β1* in adipose tissue parallels an increase in inflammatory and fibrosis scores in liver biopsies. In human adipose tissue cultures, an increase of TGF-β1 expression was seen when pro-inflammatory mediators TNF-α and IL-1β were inhibited through abolishment by their receptors or chelating antibodies (Fain et al., 2005). It was also noted that adipose tissue explants may undergo an up-regulation of TGF-β1 in the presence of exogenous insulin, suggesting TGF-β1 involvement in the development of insulin resistance (Fain et al., 2005). Yet TGFβ is also known to activate transcription

and translation of IL-1 and TNF-α in monocytes/macrophage precursors (reviewed in Wahl et al., 1990). The dual role of TGFβ as both a pro and anti-inflammatory mediator may have to do with a negative feedback loop regulating TGFβ expression (Wahl et al., 1990).

Importantly, the levels of TGF-β1 and TNF-α in serum were inversely correlated to each other, which is consistent with previously published results (Fain et al., 2005). Notably, the expression levels of *TGF-β1* encoding mRNA in adipose tissue were positively correlated with CSF-1 and GM-CSF, both are the markers for macrophage presence. Due to the severity of obesity in our cohort, the effects of *TGF-β1* expression maybe dampened by the chronic systematic inflammation; thus diminishing the anti-inflammatory effects of this complex, multifaceted molecule. It should be noted that TGF-β1 may act in both an autocrine and paracrine manner by binding to its receptor molecules on monocytes and inducing further TGF-β1 production, yet while doing so it may also stimulate internalization of its receptor, causing the down-regulation of surface sensitivity to TGF-β1 and decreasing the effect of TGF-β1 produced (Wahl et al., 1990). The reason that this relationship is seen in the intact human body, but not in the adipose explants from (Fain et al., 2005) may be the requirement for frequent media changes that are common in cell culturing. In this case, the inhibitory feedback on TGF-β1 production may be diminished due to removal of the produced cytokine.

In adipose, expression levels of mRNA encoding for *KCNRGv2* were shown to positively correlate with expression levels of *TGF-β1*. Accordingly, the expression levels of *KCNRGv2* encoding mRNA were inversely correlated with the scores for Kupffer cells

and PMN inflammation. The relationship seen between *TGF-β1* and *KCNRGv2* expressions levels in adipose may indicate possible involvement of TGF-β1 in cell cycle or cell size regulation. Interestingly, previous studies showed an increased expression of both TGF-β1 and TGF-β2 in porcine oocytes collected from large as compared to medium and small follicles (Jackowska et al., 2013). Also, the expression of mRNA that encodes for *KCNRGv2* decreased along with an increase in severity of liver disease. As KCNRGv2 is known for its tumor suppressor effects (Birerdinc et al., 2010), the observed decreases in its expression may be related to an increased risk of tumorigenesis that is known to be associated with morbid obesity (Fader et al., 2009; McCawley et al., 2009; Menéndez et al., 2012).

We also noted that patients with NASH expressed lower levels of mRNAs encoding for *PRDM16* and *UCP1*, known indicators of brown adipose tissue (BAT) activation. This observation may provide insight into possible anti-inflammatory properties of BAT or beige infiltrates within VAT. It appears that expression levels of mRNAs encoding for *UCP1* and *TGF-β1* are correlated, and may perhaps regulate each other. Based on the data from our morbidly obese cohort, expression levels of mRNAs encoding for *UCP1* may be regulated in a gender specific manner, thus, possibly indicating that visceral adipose depots of females contains more interspersed brown adipose cells. There might be a number of explanations to those gender specific differences, for example, having BAT in adipose depots near the wombs of females would have undoubtedly given a selective advantage in providing additional warmth to developing embryos. Gender-specific differences in amounts of interspersed brown

adipocytes could be contributing to previously noted buffering of the morbid effects of obesity seen in females (Lönnqvist et al., 1997).

Importantly, visceral adipose expression levels of mRNAs encoding for *PRDM16* and *UCP1* were positively correlated with expression levels of mRNAs encoding for various transcription factors and other important genes, for example, *TBX21, CD3E, GATA3, TGF-βR1, TGF-β1,* and *KCNRGv2*. Those genes could influence the expression and differentiation of BAT through a variety of pathways. Further studies are warranted to conclusively dissect their relative involvement and influence on the differentiation and functioning of interspersed BAT within the visceral adipose depots.

Limitations of Current Study

The amounts of brown adipocytes interspersed within the visceral adipose depots are relatively small. In the bulk of adipose tissue, these cells contribute only to a fraction of total RNA. Genes expressed at very low levels were difficult to reliably analyze. Some transcripts, especially those encoding for the BAT specific markers *UCP1* and *PRDM16*, would not amplify at template amounts lower than 1 ng/uL of cDNA. These transcripts were equally rare in the universal template composed of various human tissue mRNAs. Similar problems were encountered with amplifications of mRNA encoding for T-cell transcription factors *FOXP3* and *TBX21*.

Another possible variable of concern in this research would be the type of liver biopsy obtained. There are two main ways to collect a liver biopsies, core needle and wedge (Mirza, 2011). The core needle approach collects a smaller area of sample compared to the wedge method. To minimize the damage to the patients' livers, INOVA

hospital utilizes the core needle liver biopsy approach. Core needle biopsies are known to be biased; they may or may not reflect the overall condition of the patient's liver. The liver, especially during early stages of disease, may not be homogenous. This could lead to discrepancies in classification and diagnosis of liver disease (Mirza, 2011).

CONCLUSIONS

Our study demonstrated that the influence of the cytokines on the expression of other genes and inflammatory features in various organs is highly complex and the majority of relationships are interdependent. For example, TGF-β1 is known to initiate macrophage activation and production of pro-inflammatory mediators. Overall, the visceral adipose expression levels of mRNA encoding for *TGF-β1* decreased with an increase in histological scores for liver inflammation and fibrosis. It seems that in adipose the down-regulation of *TGF-β1* may be explained by an engagement of an inhibitory feedback loop that may act to partially alleviate the systemic action of pro-inflammatory cytokines such as IL-13, IL-1β, and TNF-α increased along with a progression of liver inflammation. In adipose tissue, the levels of *TGF-β1* were also positively correlated with that of mRNA encoding for BAT biomarkers *PRDM16* and *UCP1*. Thus, our study provided evidence on the complexity of TGF-β1 expression, and how it influences the inflammatory and tissue repair processes. We also showed that the expression levels of mRNAs encoding for *UCP1* may be regulated in a gender specific manner.

REFERENCES

Ahonen, T.M., Saltevo, J.T., Kautiainen, H.J., Kumpusalo, E.A., and Vanhala, M.J. (2012). The association of adiponectin and low-grade inflammation with the course of metabolic syndrome. Nutr. Metab. Cardiovasc. Dis. NMCD *22*, 285–291.

Amento, E.P., Ehsani, N., Palmer, H., and Libby, P. (1991). Cytokines and growth factors positively and negatively regulate interstitial collagen gene expression in human vascular smooth muscle cells. Arterioscler. Thromb. Vasc. Biol. *11*, 1223–1230.

Arita, Y., Kihara, S., Ouchi, N., Takahashi, M., Maeda, K., Miyagawa, J., Hotta, K., Shimomura, I., Nakamura, T., Miyaoka, K., et al. (1999). Paradoxical Decrease of an Adipose-Specific Protein, Adiponectin, in Obesity. Biochem. Biophys. Res. Commun. *257*, 79–83.

Bellisari, A. (2008). Evolutionary origins of obesity. Obes. Rev. *9*, 165–180.

Birerdinc, A., Nohelty, E., Marakhonov, A., Manyam, G., Panov, I., Coon, S., Nikitin, E., Skoblov, M., Chandhoke, V., and Baranova, A. (2010). Pro-apoptotic and antiproliferative activity of human KCNRG, a putative tumor suppressor in 13q14 region. Tumour Biol. J. Int. Soc. Oncodevelopmental Biol. Med. *31*, 33–45.

Birerdinc, A., Jarrar, M., Stotish, T., Randhawa, M., and Baranova, A. (2013). Manipulating molecular switches in brown adipocytes and their precursors: A therapeutic potential. Prog. Lipid Res. *52*, 51–61.

Bjorndal, B., Burri, L., Staalesen, V., Skorve, J., and Berge, R.K. (2011). Different Adipose Depots: Their Role in the Development of Metabolic Syndrome and Mitochondrial Response to Hypolipidemic Agents. J. Obes. *2011*.

Bondini, S., Kallman, J., Wheeler, A., Prakash, S., Gramlich, T., Jondle, D.M., and Younossi, Z.M. (2007). Impact of non-alcoholic fatty liver disease on chronic hepatitis B. Liver Int. *27*, 607–611.

Cannon, B., and Nedergaard (2004). Brown Adipose Tissue: Function and Physiological Significance. Physiol. Rev. *84*, 277–359.

Cao, H. (2014). Adipocytokines in obesity and metabolic disease. J. Endocrinol. *220*, T47–59.

Cinti, S. (2009). Reversible physiological transdifferentiation in the adipose organ. Proc. Nutr. Soc. *68*, 340–349.

Cinti, S. (2012). The adipose organ at a glance. Dis. Model. Mech. *5*, 588–594.

Cinti, S., Mitchell, G., Barbatelli, G., Murano, I., Ceresi, E., Faloia, E., Wang, S., Fortier, M., Greenberg, A.S., and Obin, M.S. (2005). Adipocyte death defines macrophage localization and function in adipose tissue of obese mice and humans. J. Lipid Res. *46*, 2347–2355.

Cipolletta, D., Kolodin, D., Benoist, C., and Mathis, D. (2011). Tissular Tregs: A unique population of adipose-tissue-resident Foxp3+CD4+ T cells that impacts organismal metabolism. Semin. Immunol. *23*, 431–437.

Cypess, A.M., Lehman, S., Williams, G., Tal, I., Rodman, D., Goldfine, A.B., Kuo, F.C., Palmer, E.L., Tseng, Y.-H., and Doria, A. (2009). Identification and importance of brown adipose tissue in adult humans. N. Engl. J. Med. *360*, 1509–1517.

Fader, A.N., Arriba, L.N., Frasure, H.E., and von Gruenigen, V.E. (2009). Endometrial cancer and obesity: epidemiology, biomarkers, prevention and survivorship. Gynecol. Oncol. *114*, 121–127.

Fain, J.N., Tichansky, D.S., and Madan, A.K. (2005). Transforming Growth Factor β1 release by human adipose tissue is enhanced in obesity. Metabolism *54*, 1546–1551.

Feuerer, M., Herrero, L., Cipolletta, D., Naaz, A., Wong, J., Nayer, A., Lee, J., Goldfine, A.B., Benoist, C., Shoelson, S., et al. (2009). Lean, but not obese, fat is enriched for a unique population of regulatory T cells that affect metabolic parameters. Nat. Med. *15*, 930–939.

Finkelstein, E.A., Khavjou, O.A., Thompson, H., Trogdon, J.G., Pan, L., Sherry, B., and Dietz, W. (2012). Obesity and Severe Obesity Forecasts Through 2030. Am. J. Prev. Med. *42*, 563–570.

Goktas, Z., Moustaid-Moussa, N., Shen, C.-L., Boylan, M., Mo, H., and Wang, S. (2013). Effects of bariatric surgery on adipokine-induced inflammation and insulin resistance. Diabetes *4*, 69.

Gutierrez, D.A., Puglisi, M.J., and Hasty, A.H. (2009). Impact of Increased Adipose Tissue Mass on Inflammation, Insulin Resistance, and Dyslipidemia. Curr. Diab. Rep. *9*, 26–32.

Han, S.H., Yea, S.S., Jeon, Y.J., Yang, K.-H., and Kaminski, N.E. (1998). Transforming Growth Factor-Beta 1 (TGF-β1) Promotes IL-2 mRNA Expression Through the Up-

regulation of NF-κB, AP-1 and NF-AT in EL4 Cells. J. Pharmacol. Exp. Ther. *287*, 1105–1112.

Harrington, L.E., Hatton, R.D., Mangan, P.R., Turner, H., Murphy, T.L., Murphy, K.M., and Weaver, C.T. (2005). Interleukin 17-producing CD4+ effector T cells develop via a lineage distinct from the T helper type 1 and 2 lineages. Nat. Immunol. *6*, 1123–1132.

Hornigold, N., Johnson, T.S., Huang, L., Haylor, J.L., Griffin, M., and Mooney, A. (2013). Inhibition of collagen I accumulation reduces glomerulosclerosis by a Hic-5-dependent mechanism in experimental diabetic nephropathy. Lab. Investig. J. Tech. Methods Pathol. *93*, 553–565.

Hosogai, N., Fukuhara, A., Oshima, K., Miyata, Y., Tanaka, S., Segawa, K., Furukawa, S., Tochino, Y., Komuro, R., Matsuda, M., et al. (2007). Adipose tissue hypoxia in obesity and its impact on adipocytokine dysregulation. Diabetes *56*, 901–911.

Jackowska, M., Kempisty, B., Woźna, M., Piotrowska, H., Antosik, P., Zawierucha, P., Bukowska, D., Nowicki, M., Jaśkowski, J.M., and Brüssow, K.-P. (2013). Differential expression of GDF9, TGFB1, TGFB2 and TGFB3 in porcine oocytes isolated from follicles of different size before and after culture in vitro. Acta Vet. Hung. *61*, 99–115.

Kang, S.-W., Kim, M.S., Kim, H.-S., Kim, Y., Shin, D., Park, J.H.Y., and Kang, Y.-H. (2013). Celastrol attenuates adipokine resistin-associated matrix interaction and migration of vascular smooth muscle cells. J. Cell. Biochem. *114*, 398–408.

Kintscher, U., Hartge, M., Hess, K., Foryst-Ludwig, A., Clemenz, M., Wabitsch, M., Fischer-Posovszky, P., Barth, T.F.E., Dragun, D., Skurk, T., et al. (2008). T-lymphocyte Infiltration in Visceral Adipose Tissue A Primary Event in Adipose Tissue Inflammation and the Development of Obesity-Mediated Insulin Resistance. Arterioscler. Thromb. Vasc. Biol. *28*, 1304–1310.

Lean, M.E., James, W.P., Jennings, G., and Trayhurn, P. (1986). Brown adipose tissue uncoupling protein content in human infants, children and adults. Clin. Sci. Lond. Engl. 1979 *71*, 291–297.

Lee, K.-Y., Kang, H.-S., and Shin, Y.-A. (2013). Exercise improves adiponectin concentrations irrespective of the adiponectin gene polymorphisms SNP45 and the SNP276 in obese Korean women. Gene *516*, 271–276.

Lönnqvist, F., Thörne, A., Large, V., and Arner, P. (1997). Sex differences in visceral fat lipolysis and metabolic complications of obesity. Arterioscler. Thromb. Vasc. Biol. *17*, 1472–1480.

Luyckx, F.H., Lefebvre, P.J., and Scheen, A.J. (2000). Non-alcoholic steatohepatitis: association with obesity and insulin resistance, and influence of weight loss. Diabetes Metab. *26*, 98–106.

Malis, C., Rasmussen, E.L., Poulsen, P., Petersen, I., Christensen, K., Beck-Nielsen, H., Astrup, A., and Vaag, A.A. (2005). Total and regional fat distribution is strongly influenced by genetic factors in young and elderly twins. Obes. Res. *13*, 2139–2145.

McCawley, G.M., Ferriss, J.S., Geffel, D., Northup, C.J., and Modesitt, S.C. (2009). Cancer in obese women: potential protective impact of bariatric surgery. J. Am. Coll. Surg. *208*, 1093–1098.

McGown, C., Birerdinc, A., and Younossi, Z.M. (2014). Adipose tissue as an endocrine organ. Clin. Liver Dis. *18*, 41–58.

Mehta, R., Birerdinc, A., Hossain, N., Afendy, A., Chandhoke, V., Younossi, Z., and Baranova, A. (2010). Validation of endogenous reference genes for qRT-PCR analysis of human visceral adipose samples. BMC Mol. Biol. *11*, 39.

Menéndez, P., Padilla, D., Villarejo, P., Menéndez, J.M., and Lora, D. (2012). Does bariatric surgery decrease gastric cancer risk? Hepatogastroenterology. *59*, 409–412.

Miao, C., Yang, Y., He, X., Huang, C., Huang, Y., Zhang, L., Lv, X.-W., Jin, Y., and Li, J. (2013). Wnt signaling in liver fibrosis: Progress, challenges and potential directions. Biochimie *95*, 2326–2335.

Mikhail Skoblov, A.M. (2013). Protein partners of KCTD proteins provide insights about their functional roles in cell differentiation and vertebrate development. BioEssays News Rev. Mol. Cell. Dev. Biol.

Mirza, M.S. (2011). Obesity, Visceral Fat, and NAFLD: Querying the Role of Adipokines in the Progression of Nonalcoholic Fatty Liver Disease. ISRN Gastroenterol. *2011*.

Nedergaard, J., Bengtsson, T., and Cannon, B. (2007). Unexpected evidence for active brown adipose tissue in adult humans. Am. J. Physiol. - Endocrinol. Metab. *293*, E444–E452.

O'Garra, A. (1998). Cytokines Induce the Development Review of Functionally Heterogeneous T Helper Cell Subsets. Immunity *8*, 275–283.

Orava, J., Nuutila, P., Lidell, M.E., Oikonen, V., Noponen, T., Viljanen, T., Scheinin, M., Taittonen, M., Niemi, T., Enerbäck, S., et al. (2011). Different Metabolic Responses of Human Brown Adipose Tissue to Activation by Cold and Insulin. Cell Metab. *14*, 272–279.

Petrovic, N., Walden, T.B., Shabalina, I.G., Timmons, J.A., Cannon, B., and Nedergaard, J. (2010). Chronic Peroxisome Proliferator-activated Receptor-Y (PPAR-Y) Activation of Epididymally Derived White Adipocyte Cultures Reveals a Population of Thermogenically Competent, UCP1-containing Adipocytes Molecularly Distinct from Classic Brown Adipocytes. J. Biol. Chem. *285*, 7153–7164.

Sadashiv (2012). Over expression of resistin in adipose tissue of the obese induces insulin resistance. World J. Diabetes *3*, 135.

Silventoinen, K., Sans, S., Tolonen, H., Monterde, D., Kuulasmaa, K., Kesteloot, H., Tuomilehto, J., and WHO MONICA Project (2004). Trends in obesity and energy supply in the WHO MONICA Project. Int. J. Obes. Relat. Metab. Disord. J. Int. Assoc. Study Obes. *28*, 710–718.

Stefan, N., Häring, H.-U., Hu, F.B., and Schulze, M.B. (2013). Metabolically healthy obesity: epidemiology, mechanisms, and clinical implications. Lancet Diabetes Endocrinol. *1*, 152–162.

Szabo, S.J., Glimcher, L.H., and Ho, I. (1997). Genes that regulate interleukin-4 expression in T cells. Curr. Opin. Immunol. *9*, 776–781.

Taylor, R. (1990). Interpretation of the correlation coefficient: a basic review. J. Diagn. Med. Sonogr. *6*, 35–39.

Ting, C.N., Olson, M.C., Barton, K.P., and Leiden, J.M. (1996). Transcription factor GATA-3 is required for development of the T-cell lineage. Nature *384*, 474–478.

Townsend, K., and Tseng, Y.-H. (2012). Brown adipose tissue. Adipocyte *1*, 13–24.

Valenti, L., Rametta, R., Ruscica, M., Dongiovanni, P., Steffani, L., Motta, B.M., Canavesi, E., Fracanzani, A.L., Mozzi, E., and Roviaro, G. (2012). The i148m Pnpla3 polymorphism influences serum adiponectin in patients with fatty liver and healthy controls. BMC Gastroenterol. *12*, 111.

Virtanen, K.A., Lidell, M.E., Orava, J., Heglind, M., Westergren, R., Niemi, T., Taittonen, M., Laine, J., Savisto, N.-J., and Enerbäck, S. (2009). Functional brown adipose tissue in healthy adults. N. Engl. J. Med. *360*, 1518–1525.

Wahl, S.M., McCartney-Francis, N., Allen, J.B., Dougherty, E.B., and Dougherty, S.F. (1990). Macrophage Production of TGF-β and Regulation by TGF-β. Ann. N. Y. Acad. Sci. *593*, 188–196.

Wang, F., Deeney, J.T., and Denis, G.V. (2013). Brd2 gene disruption causes “metabolically healthy” obesity: Epigenetic and chromatin-based mechanisms that uncouple obesity from Type 2 diabetes. Vitam. Horm. *91*, 49–75.

Weisberg, S.P., Hunter, D., Huber, R., Lemieux, J., Slaymaker, S., Vaddi, K., Charo, I., Leibel, R.L., and Ferrante, A.W. (2006). CCR2 modulates inflammatory and metabolic effects of high-fat feeding. J. Clin. Invest. *116*, 115–124.

Wu, J., Boström, P., Sparks, L.M., Ye, L., Choi, J.H., Giang, A.-H., Khandekar, M., Virtanen, K.A., Nuutila, P., Schaart, G., et al. (2012). Beige Adipocytes Are a Distinct Type of Thermogenic Fat Cell in Mouse and Human. Cell *150*, 366–376.

Zajac, E., Schweighofer, B., Kupriyanova, T.A., Juncker-Jensen, A., Minder, P., Quigley, J.P., and Deryugina, E.I. (2013). Angiogenic capacity of M1- and M2-polarized macrophages is determined by the levels of TIMP-1 complexed with their secreted proMMP-9. Blood *122*, 4054–4067.

Zheng, W., and Flavell, R.A. (1997). The transcription factor GATA-3 is necessary and sufficient for Th2 cytokine gene expression in CD4 T cells. Cell *89*, 587–596.

CURRICULUM VITAE

Maria Ashley Keaton graduated from Brentsville District High School in Nokesville, Virginia, in 2006. She received her Associate of Science from Northern Virginia Community College in 2008 and later received her Bachelor of Science from James Madison University in 2010. She currently volunteers at INOVA Fairfax Hospital in the Betty and Guy Beatty Center for Integrated Research where she also works as a graduate research assistant for Dr. Baranova.